PROGRAM ON APPLICATION OF COMMUNICATIONS SATELLITES
TO EDUCATIONAL DEVELOPMENT

WASHINGTON UNIVERSITY

Report No. T-71/3 May, 1971

WIDEBAND CW MICROWAVE AMPLIFICATION USING GUNN EFFECT DEVICES

Amadou Sene

Fred J. Rosenbaum

This research is supported by the National Aeronautics and Space Administration under Grant No. Y/NGL-26-008-054 and it does not necessarily represent the views of either the research team as a whole or NASA.

PROGRAM ON APPLICATION OF COMMUNICATIONS SATELLITES
TO EDUCATIONAL DEVELOPMENT

WASHINGTON UNIVERSITY

Report No. T-71/3 May, 1971

WIDEBAND CW MICROWAVE AMPLIFICATION USING GUNN EFFECT DEVICES

Amadou Sene

Fred J. Rosenbaum

This research is supported by the National Aeronautics and Space Administration under Grant No. Y/NGL-26-008-054 and it does not necessarily represent the views of either the research team as a whole or NASA.

ABSTRACT

The Gunn Effect has been used mainly for oscillator applications. Recently, the negative resistance properties of the Gunn diode have been used in reflection-type amplifiers. All the published work has been done in coaxial and microstrip circuits. This work extends the applications to waveguide circuitry. Broadband gains exceeding 10dB over a 1GHz bandwidth have been obtained. An equivalent circuit for the amplifier is proposed. Using experimental data on the phase and magnitude of the reflection coefficient and the equivalent circuit, the impedance of the diode is calculated. It is found that the equivalent series resistance is constant over a 1.8GHz bandwidth at -30Ω at 6.5 volts bias, and at -40Ω at 7.0 volts over a 1.2GHz band. Gain simulation on computer indicates that a series model for the diode gives good agreement with experimental data.

The performance of the amplifier is characterized. A 94dB linear dynamic range at a gain of 28dB has been measured. Saturation beginning at -8dBm input power is typical of the low power diodes used. The noise figure measured at 10dB gain was 24dB.

TABLE OF CONTENTS

TABLE OF CONTENTS
(continued)

TABLE OF CONTENTS
(continued)

LIST OF FIGURES

LIST OF FIGURES
(continued)

LIST OF FIGURES
(continued)

WIDEBAND CW MICROWAVE AMPLIFICATION USING GUNN EFFECT DEVICES

1. INTRODUCTION

1.1 HISTORICAL BACKGROUND

The possibility of broadband amplification using bulk negative resistance effects in semiconductors was first proposed by Kroemer (1)* in 1958. The physical principle of the so-called "negative mass amplifier" (2) is that when a high electric field is applied to a suitable semiconductor, the kinetic energy of the charge carriers is such that their effective mass becomes negative. When a microwave signal is applied to the semiconductor, the charge carriers give up part of their kinetic energy to the applied field.

Experimental verification of the proposed amplifier is still lacking.

In 1961, Ridley and Watkins (3) suggested that bulk negative resistance could exist in a semiconductor due to

*The numbers in parentheses in the text indicate references in the Bibliography.

a relative change in carrier effective mass. Such a change occurs with a field dependent transfer of carriers from a high mobility valley to an adjacent, higher energy, low mobility valley. Hilsum independently proposed that GaAs would exhibit bulk negative resistance effects (4). In 1963, J. B. Gunn observed current instabilities in GaAs, InP and other Group III-V compounds (5). What Gunn observed was that, when the bias voltage across an n-type GaAs sample exceeded a certain value, the sample current broke into oscillation. The frequency of the coherent oscillation was in the microwave spectrum and about equal to the inverse of the transit time of the carriers across the sample. In a capacitive probe experiment, Gunn showed that the oscillation in the sample current was due to the transit of high-field domains in the active region (6).

In their paper (3), Ridley and Watkins mentioned that under bulk negative resistance conditions, the semiconductor would be unstable because domains of high electric field are nucleated. That the mechanism proposed by Ridley and Watkins and also Hilsum is behind the instabilities now known under the names of Gunn effect or Transferred Electron effect, was shown by Kroemer (7).

Experimental verification of the transferred electron mechanism was first obtained by Hutson et al. (8), who observed a reduction of the threshold field for the start of oscillations when the energy separation between the low and

high mobility valleys is reduced by hydrostatic pressure. A similar experiment was reported by Allen et al. (9), who used $GaAs_x P_{1-x}$ alloys to produce the reduction in intervalley energy separation.

Since then much research has been done to make the Gunn device a very useful microwave component in oscillator applications and more recently in broadband amplifiers.

Since in this work we are interested in the amplifying properties of Gunn devices, very little will be said about their behavior as oscillators. The interested reader is referred to the abundant literature and particularly to the work of Tsai (10).

1.2 PHYSICAL PRINCIPLES OF GUNN EFFECT AMPLIFIERS

Amplification in Gunn effect devices is due to an equivalent negative resistance exhibited by the device under certain conditions. The behavior of this negative resistance is governed by the equations of space charge dynamics in the semiconductor, the boundary conditions imposed by the cathode and anode of the device, and by the external microwave circuit. The basic equations in the Gunn effect are Poisson's equation and the continuity equation; assuming a one-dimensional case, they are

$$\nabla \cdot \vec{E}(x,t) = \frac{e}{\varepsilon} [n(x,t) - n_0] \qquad (1\text{-}1)$$

$$\nabla \cdot \vec{J}(x,t) = 0 \qquad (1\text{-}2)$$

where:

$E(x,t)$ = the electric field in the sample

n_0 = the background donor density

$n(x,t)$ = the electron density

e = the charge of an electron = 1.6×10^{-19} Coulombs

ε = the permittivity of the material

$\vec{J}(x,t)$ = the total current density

The total current $\vec{J}(x,t)$ has two components: the conduction current, given by

$$\vec{J}_c = ev(E)n(x,t) - e\nabla[Dn(x,t)] \qquad (1\text{-}3)$$

and the displacement current, given by

$$\vec{J}_D = \varepsilon \frac{\partial E(x,t)}{\partial t} \qquad (1\text{-}4)$$

where

$v(E)$ = average velocity of the electrons as a function of the electric field

D = the diffusion constant

The velocity-field curve is shown in Figure 1.

The total current is:

$$J(t) = ev(E)n(x,t) - e\nabla(Dn) + \varepsilon \frac{\partial \vec{E}(x,t)}{\partial t} \qquad (1\text{-}5)$$

By solving equations (1-1), (1-2), and (1-5), one can derive the equivalent impedance or admittance of the semiconductor chip. However, the above equations are nonlinear and some simplifying assumptions are necessary in order to make their solution tractable.

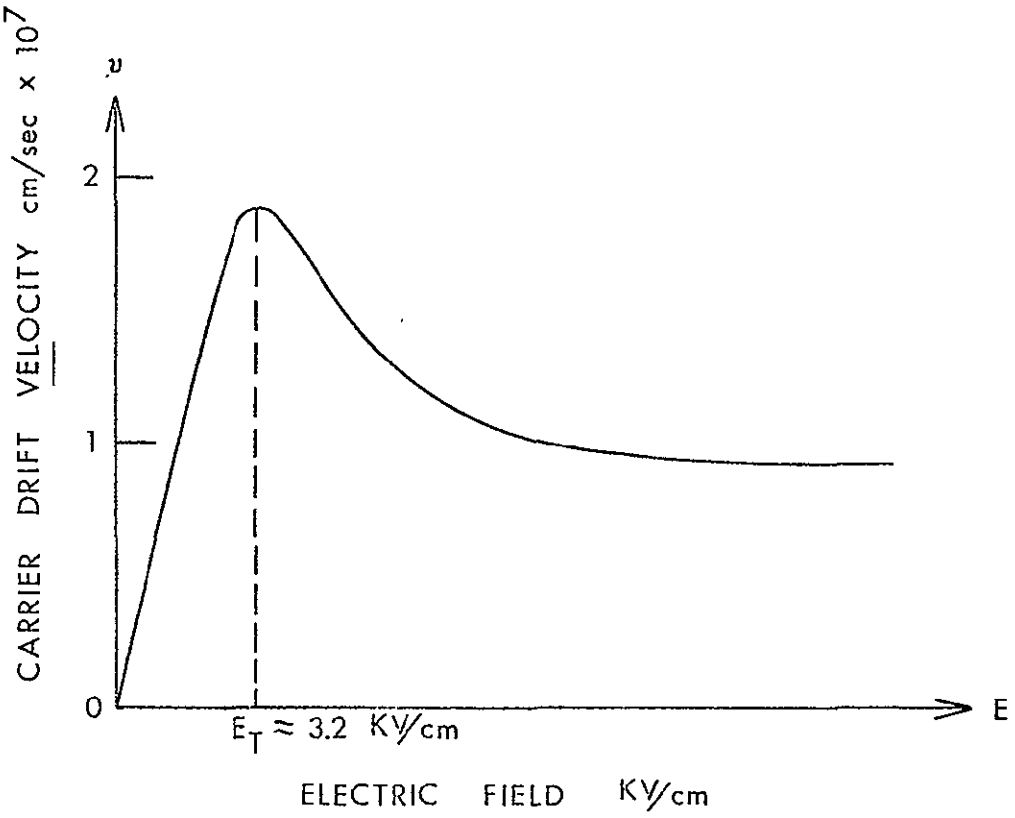

Figure 1. Average Carrier Drift Velocity Versus Electric Field for n-type GaAs

1.2.1 The McCumber-Chynoweth Model

McCumber and Chynoweth (11) have made a theoretical study of Gunn effect dynamics defined by equations (1-1), (1-2) and (1-3) using a two valley model in which the electron density in the valleys is controlled by an average electron temperature. A small signal computation of the semiconductor chip impedance, using several simplifying assumptions, yields:

$$Z(\omega) = \frac{L^2}{Ak\bar{v}} \frac{e^{-s} + s - 1}{s^2} \qquad (1\text{-}6)$$

where

$s = L(\bar{\xi} - i\omega)/\bar{v}$

ω = frequency (rad/sec)

$\bar{v}$ = drift velocity of carriers assumed constant

L = device length

k = dielectric constant of semiconductor. For GaAs, k = 12.5.

A = cross section of semiconductor chip

$\bar{\xi}$ is a voltage dependent parameter related to the slope of the velocity-field characteristics of the semiconductor and the doping density:

$$\bar{\xi} = \frac{en(x)}{k} \frac{\partial \bar{v}(E,x)}{\partial E(x)} \qquad (1\text{-}7)$$

As shown in Figure 1, $\partial\bar{v}/\partial E$ is negative in the negative mobility range above the threshold field, E_{th}.

Equation (1-6) is well behaved in the ω-plane since it has no singularities there. So the Gunn diode is stable under constant current conditions. But the admittance of the device, $Y(\omega) = 1/Z(\omega)$ has poles which correspond to the zeroes of $Z(\omega)$. The first zero of Equation (1-6) in the ω-plane occurs at

$$\omega_n = \pm 7.46 \frac{\bar{v}}{L} - i(\bar{\xi} + 2.09 \frac{\bar{v}}{L}) \qquad (1\text{-}8)$$

A stability condition under constant voltage conditions can therefore be derived from equation (1-8) at room temperature. $Y(\omega)$ must be regular in the upper half plane, that is, the imaginary part of ω must be positive (12). So the device is stable as long as

$$\bar{\xi} > - 2.09 \frac{\bar{v}}{L} \qquad (1\text{-}9)$$

or

$$n_0 L < 2.7 \times 10^{11} \text{ cm}^{-2} .$$

This upper bound is slightly less than experimentally observed values. When the effects of diffusion are included into the calculations, the upper limit is found to be about

$$n_0 L < 5.0 \times 10^{11} \text{ cm}^{-2} . \qquad (1\text{-}10)$$

1.2.2 Subcritically-Doped Amplifiers

Gunn diodes whose nL product is less than 5×10^{11} cm^{-2} are herewith referred to as being subcritically doped. They

are inherently stable since when biased above threshold, they do not exhibit the type of current instabilities (high-field domains) originally observed by Gunn. To see this, let us consider space-charge growth in the Gunn effect. Kroemer (13) has shown that the equation describing space charge growth is

$$Q(t) = Q(0)\, e^{-\frac{t}{T_D}} \tag{1-11}$$

where T_D is the dielectric relaxation time

$$T_D = \frac{\varepsilon}{nq\mu} \tag{1-12}$$

where

n = the doping density

q = electron charge (assumed positive)

μ = the mobility of the electrons below threshold, in the region of positive dv/dE.

In the negative mobility region, T_D is negative (14). Thus, starting at the cathode, the space charge grows exponentially as it moves toward the anode. As it grows the electric field inside the space charge region increases. Eventually the space-charge grows into a mature dipole. But if the length of the device, L, is such that the transit time is less than the time constant, T_D, a mature dipole is not formed before the space charge reaches the cathode; hence transit-time oscillations are not started. Mathematically,

$$\frac{L}{v} < \frac{\varepsilon}{nq\mu} \qquad (1\text{-}13)$$

or

$$nL < \frac{v\varepsilon}{\mu q} \qquad (1\text{-}14)$$

For GaAs, if we let $v = 10^7$ cm/sec, $\mu = 100$ cm^2/v.s., we find

$$nL < 6.9 \times 10^{11} \text{ cm}^{-2}$$

which is in close agreement with equation (1-10).

If equation (1-6) is separated into a real and an imaginary part, it is found that the resistance is negative around the transit time frequency (11). Such a negative resistance does not exist at lower frequencies, because the space charge is current limited (11). At any point along the sample the electric field is an increasing function of current. Hence, the i-v characteristic of such a diode does not show a negative slope region. Subcritically-doped diodes thus do not exhibit bias circuit oscillations (15). Given a suitable circuit subcritically-doped diodes can be used in reflection type amplifiers. The first such amplifier was demonstrated by Thim et al. (16) and has since raised considerable attention (17-22).

Since the negative resistance in subcritically-doped amplifiers exists only in a narrow range of frequencies, only narrow band amplifiers can be built with them.

1.2.3 Traveling Dipole Amplifiers

When the nL-product of a Gunn diode is above 5 x 10^{11} cm^{-2}, the device is supercritically doped. When biased above the threshold voltage, high-field dipole domains are nucleated near the cathode boundary. The diode oscillates in the transit-time mode or the Gunn mode.

The equivalent circuit of a Gunn diode with a high field dipole present has been calculated by Hobson (23). The equivalent circuit is shown in Figure 2. It consists of two parallel RC circuits in series. The quantities R_C and C_C are the equivalent resistance and capacitance of the part of the device outside the domain. The quantities R_D and C_D are the equivalent resistance and capacitance of the high field dipole domain. They are dependent on the bias voltage. If d is the domain width, Heinle (24) has shown that

$$R_D = \frac{d}{en\mu_2 A} \tag{1-15}$$

and

$$C_D = \frac{\varepsilon A}{d} \tag{1-16}$$

where

μ_2 = the mobility of the electrons in the negative region

n = the doping density

A = the cross-sectional area of the sample

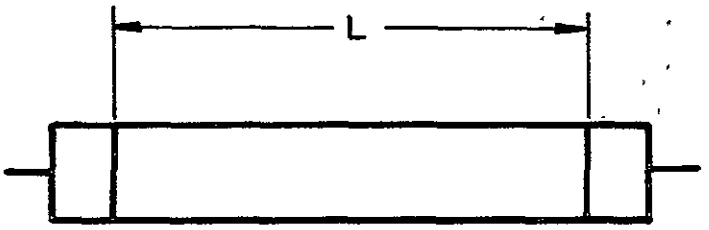

(a)

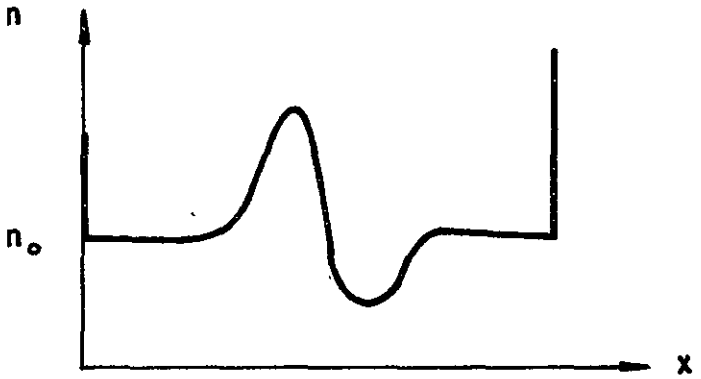

(b)

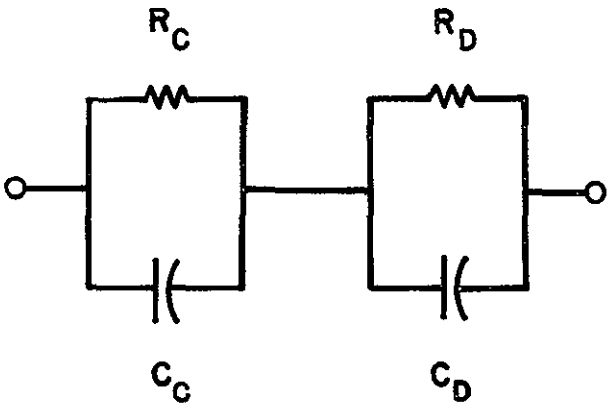

(c)

Figure 2. Equivalent Circuit of High Field Domain in Transit

The resistance R_D is negative when a dipole domain is in transit because, in the high field region, the differential mobility, μ_2, is negative. Thus a Gunn diode oscillating in the Gunn mode (transit-time) can be used as a negative resistance amplifier. This was experimentally demonstrated by Thim (25). Amplification at lower frequencies is possible. The positive series resistance, R_C, imposes an upper limit on the frequency of amplification. It is given by (26)

$$f \cdot L = \frac{\mu}{4\pi} (E_D - E_0) \qquad (1\text{-}17)$$

where E_D is the domain field, and E_0 the field outside the domain.

It is to be noted that both the domain equivalent resistance and capacitance are voltage dependent through the domain width, d. Thus the Gunn diode oscillating in transit-time mode can be used as a parametric amplifier at lower frequencies (27).

1.2.4 Supercritically-Doped Stable Amplifiers

The traveling domain amplifier of Section 1.2.3, although it has a higher power output than the subcritically-doped amplifier, has the inconvenience of operating at the same time as an oscillator.

Narayan and Sterzer (28) have shown that it is possible to stabilize a supercritically doped diode with a network in series with the device. Such an impedance stabilized

amplifier is not very broadband, since the stabilization mechanism is an extension of the McCumber-Chynoweth theory.

Perlman et al. (29), Magarshack and Micea (30) have reported on wideband, supercritically doped amplifiers. In both experiments, the Gunn diode is placed in a coaxial circuit and biased at two to three times the threshold voltage. It is believed that a combination of diffusion effects (31), temperature effects due to the reduced mobility of the carriers at high bias, the electric field across the active region, and load conditions are responsible for stabilizing the diode. As shown before, the time required for domain formation in a Gunn diode is approximately given by equation (1-11):

$$T_D = \frac{\varepsilon}{nq|\mu|}$$

A fully grown domain will not form if T_D is less than the transit time L/v_D. At twice to three times the threshold voltage $|\mu|$ is very small, so T_D is large: Hence, in short devices a domain will not form; only an accumulation of space charge will be present, resulting in a frequency dependent negative resistance.

Perlman (32) has reported bandwidth as high as 1.76GHz at 6GHz and a noise figure of 15dB.

1.3 SCOPE OF THE PRESENT STUDY

The supercritically-doped amplifiers reported by Perlman and Magarshack were built using transmission line

structures. The objective of the present investigation is to characterize and evaluate the performance of supercritically doped amplifiers in waveguide structures at X-band (8.2 - 12.4GHz).

In Chapter 2, experimental results are evaluated. Using an equivalent circuit model for the amplifier structure, the impedance of the diode is calculated using experimental measurements of the gain and phase response of the amplifier.

In Chapter 3 the results of Chapter 2 are used to simulate the frequency response of the amplifier. A computation of the load seen by the diode is presented. The gain bandwidth limitations of the optimum negative resistance amplifier are also considered.

Chapter 4 evaluates the performance of the amplifier in terms of noise figure, dynamic range and nonlinear behavior.

2. CHARACTERIZATION OF WAVEGUIDE GUNN AMPLIFIER

2.1 INTRODUCTION

This chapter describes the use of Gunn effect devices in reflection type amplifiers in a waveguide circuit at X-band.

The amplifier circuit is described, and the frequency response is studied as the bias voltage and the temperature of the heat sink. Using these experimental results, the impedance of the diode is calculated as a function of voltage, temperature, and input power.

2.2 AMPLIFIER CIRCUIT

The experimental setup is shown in Figure 3. The output of a sweep oscillator is split by a 10dB directional coupler. The -10dB output is detected and applied to the reference input of a network analyzer. The other part of the swept output is attenuated by a level setting attenuator and amplified by the Gunn diode. A 10dB directional coupler samples the output of the amplifier, which, detected, is applied to the network analyzer. The analyzer which had previously been calibrated in dB/cm is then set to give a display of the ratio of the output of the amplifier and the reference input.

The Gunn diode is placed into a reduced-height waveguide cavity shown in Figure 4-a. The diode is shunt mounted in the reduced-height section, terminated by a sliding short circuit, which may be tuned to suppress

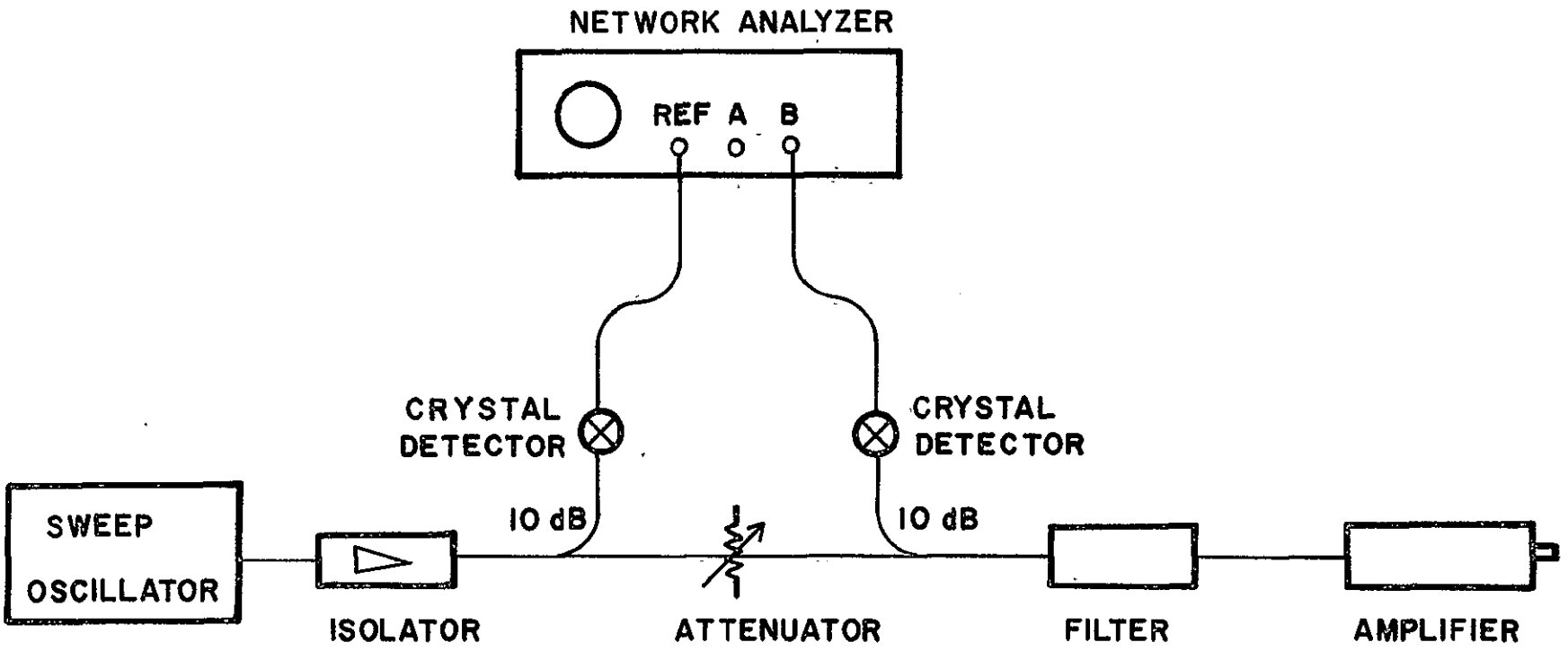

Figure 3. Experimental Setup for Amplifier

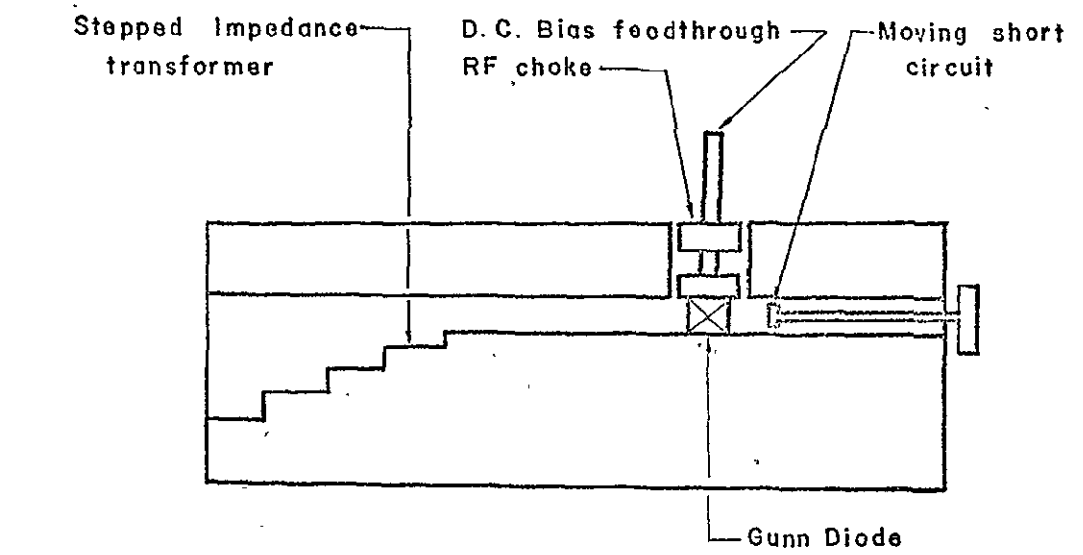

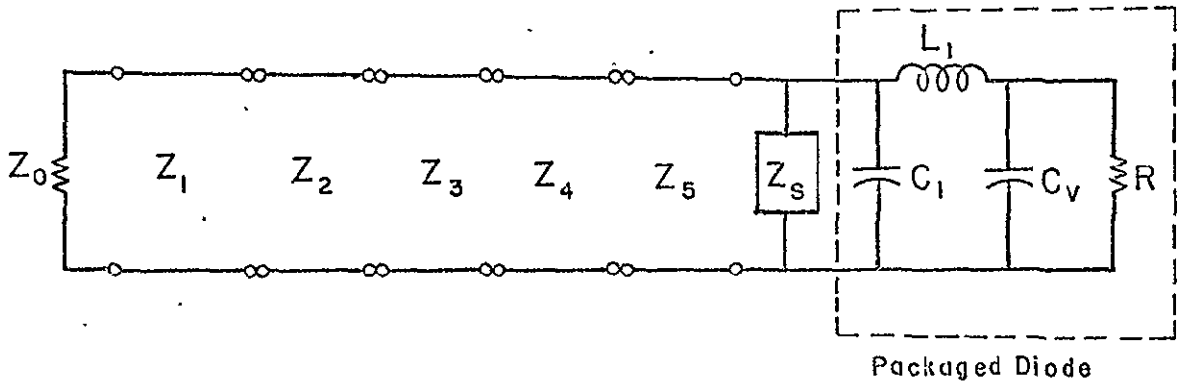

Figure 4. (a) Schematic of Amplifier Circuit
(b) Equivalent Circuit of Amplifier

oscillation and to adjust the gain. A broadband five step transformer (33) was used to match the reduced height section to the full height X-band waveguide (b = 0.400"). In this way a 6:1 reduction of the load impedance was obtained.

A schematic diagram of the amplifier equivalent circuit is shown in Figure 4-b. The input impedance of the short circuit referenced to the plane of the diode is denoted Z_s. The pill-prong diode package is represented by the shunt capacitor $C_1 \simeq 0.2$pF and the lead inductance, $L_1 = 0.5$nH. The values represent the average parasitic package capacitance and inductance of several similar packages as determined by Roe and Rosenbaum (34). Due to the distributed nature of the parasitic package parameters, it is important to measure them in the circuit in which the diode is going to be used.

The five step transformer is modeled as a cascade of five transmission lines. The VSWR of the transformer was measured to be less than 1.15 from 9 to 11GHz.

2.3 AMPLIFIER FREQUENCY RESPONSE

Using the setup of Figure 3 with Gunn diodes having nL-products of the order of 10^{12} cm^{-2} ($n \simeq 10^{15}$ cm^{-3}, $L \simeq 10$ microns), stable amplification was observed over the full X-band at several bias points.

(a)

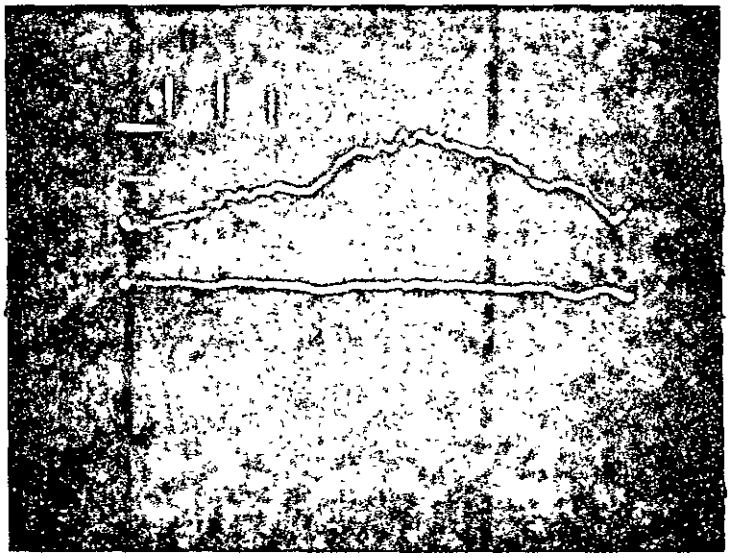

(b)

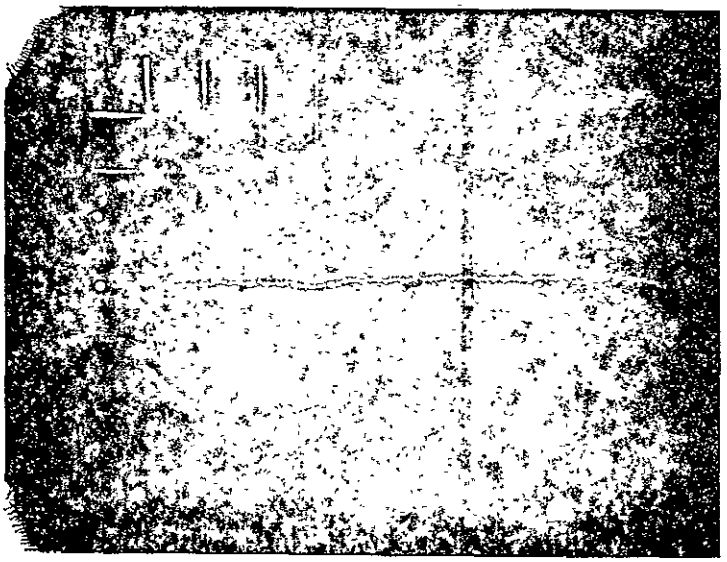

Figure 5. Frequency Response: Diode D2-39-165-4 Vertical 5dB/cm, Horizontal 8-12.4GHz, d = 0.342". Bias: a) 8V, b) 9V

2.3.1 Stabilization of the Gunn Diodes

The diodes are biased at two to three times the threshold voltage (V_{th} = 3 - 4 volts). At such high bias, the mobility of the carriers is very much reduced and fully grown dipole domains do not appear before the space-charge accumulation layer reaches the anode. The diode then presents a small signal negative resistance to the circuit. Sometimes the diode oscillates, but the load can be adjusted with the short circuit so as to suppress circuit controlled oscillations.

Since the diodes used are short (10 - 11 microns), diffusion effects are important to the stabilization mechanism (30).

Thus, supercritically doped Gunn amplifiers are stabilized by a combination of thermal effects (bias voltage, diffusion) and circuit loading.

2.3.2 Frequency Response

Several diodes were tested in the circuit for amplification. Typical responses are shown in Figure 5, for bias voltages of 8 and 9 volts and at a fixed position of the short circuit. The peak gain is 15dB. About 5dB gain is realized at band edges. The 3dB bandwidth is 1.7GHz at 8 volts.

Figure 6 shows the frequency response of another diode, 11 microns long and with a doping of 10^{15} cm^{-3} biased at 9.05 volts with the tuning short circuit at 0.475 inches.

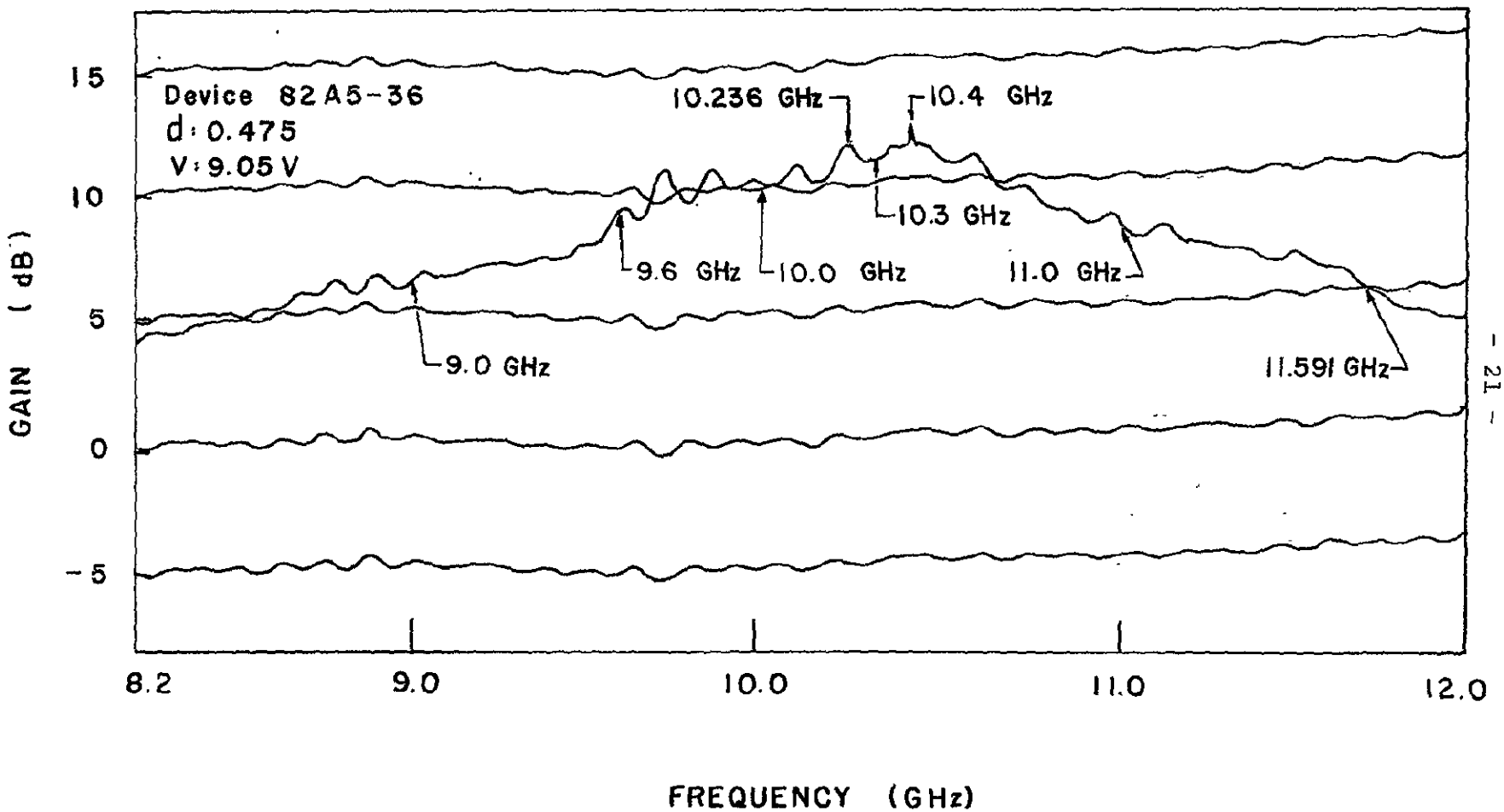

Figure 6. Frequency Response of Diode 82-A5-36 in Stepped Transformer Circuit

More than 10dB gain is observed over a 1GHz bandwidth. The 3dB bandwidth is about 1.5GHz. The drop in gain at both band edges is due to transformer VSWR degradation and also to the variations of the diode impedance with frequency.

2.3.2.a. Voltage dependence of the gain

The frequency response of the Gunn amplifier is very sensitive to bias voltage changes. Figure 7 shows the gain at three bias voltages for a fixed position of the short circuit. At frequencies below 11 GHz, the gain increases with voltage while it decreases slightly above 11GHz. At 8 volts a peak gain of 11dB is obtained over a 1.4GHz bandwidth, the corresponding 3dB bandwidth is 2GHz. Since the gain increases with the bias voltage, the 3dB bandwidth decreases. At 8.5 volts, the 3dB bandwidth is 1.2GHz, at 9 volts it is 450MHz. Thus with proper choice of bias voltage extremely wide bandwidth can be obtained with moderate gains. But the sensitivity of the frequency response to voltage changes implies in systems applications the use of highly stable power supplies. A greater freedom of choice of operation is obtained by varying the position of the short circuit. Using these two degrees of freedom one can optimize the gain bandwidth product of the amplifier.

2.3.2.b. Temperature dependence of the gain

The temperature of the diode is important to its operation as an amplifier from the point of view of stability

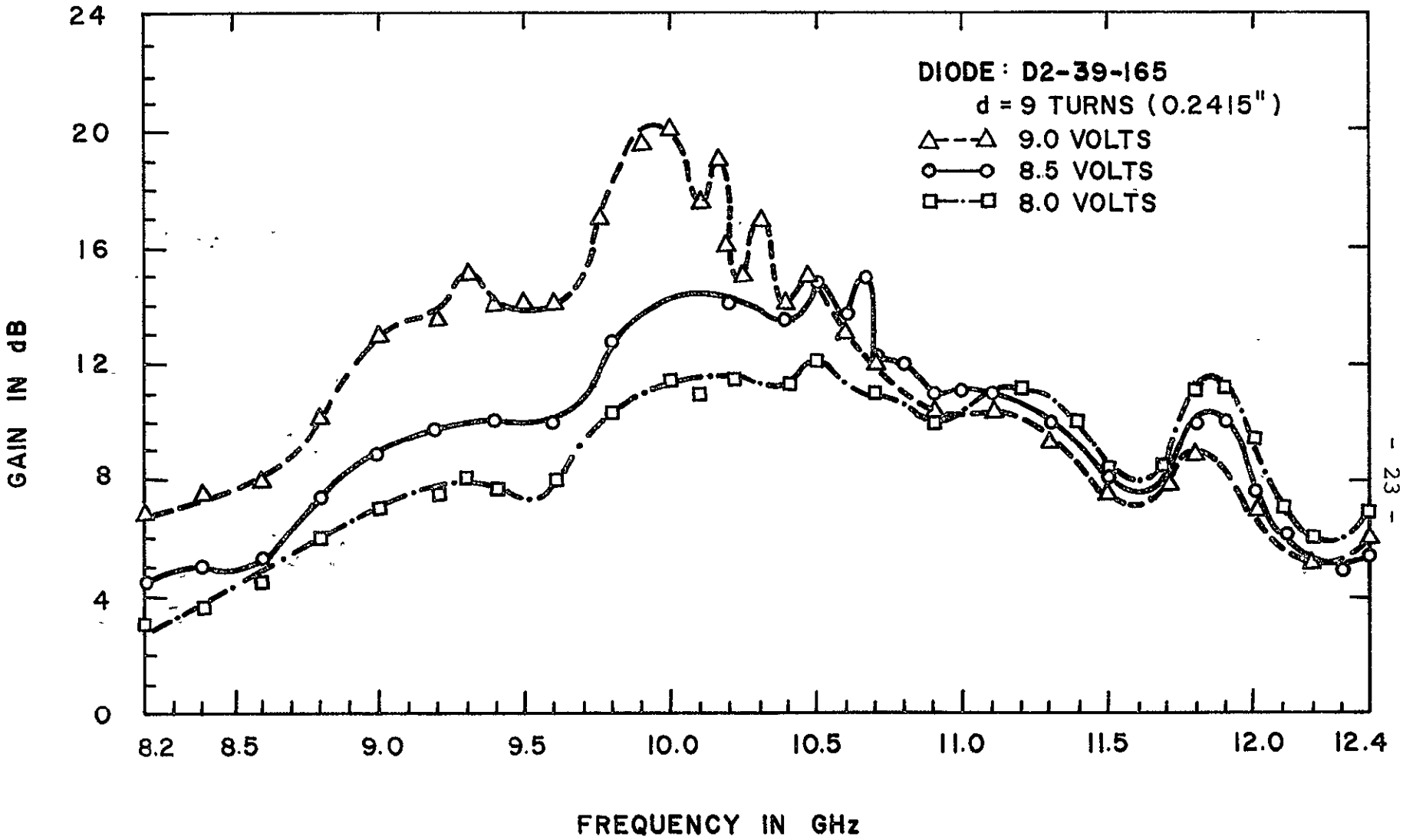

Figure 7. Gain Versus Bias Voltage

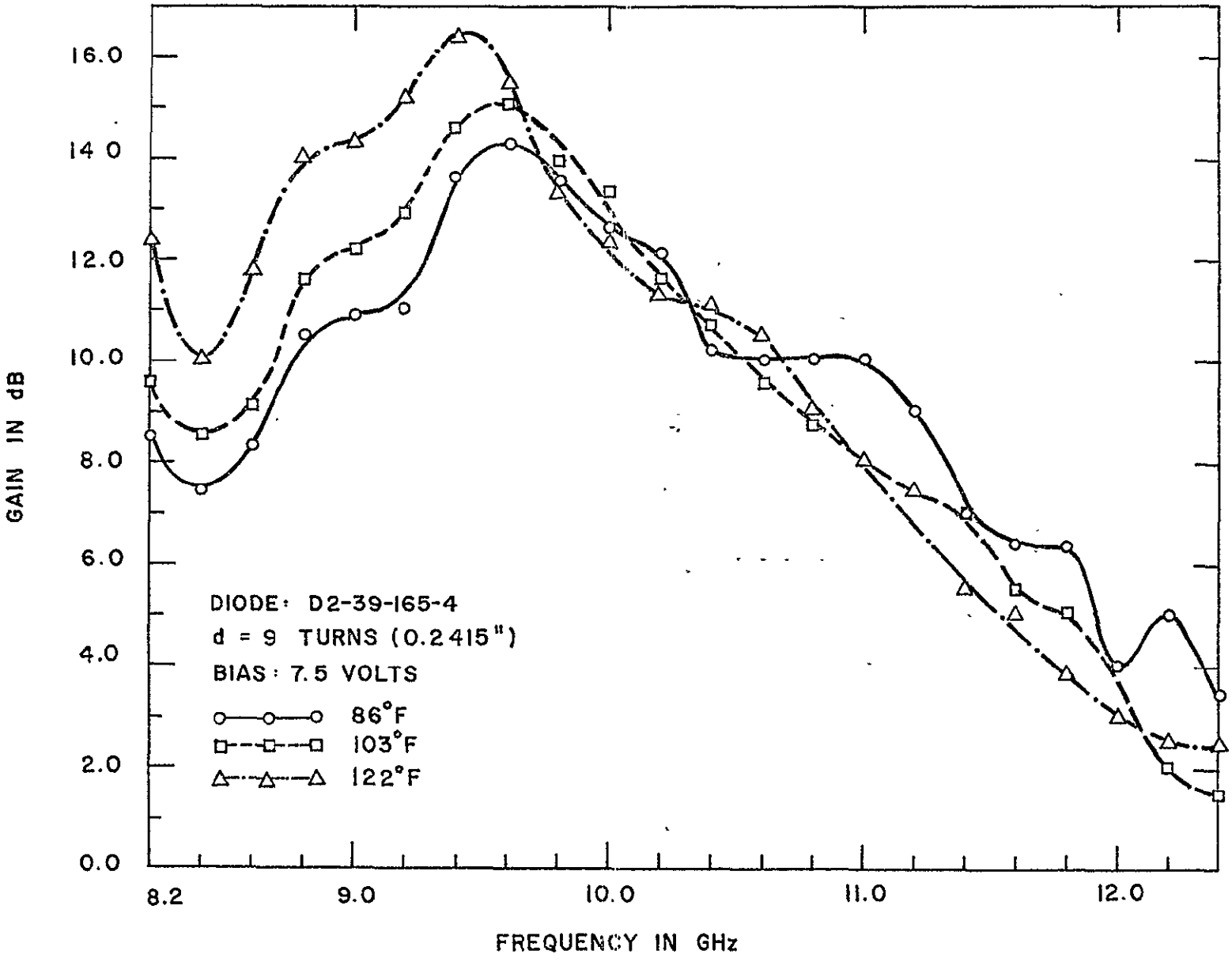

Figure 8. Gain Versus Heat Sink Temperature

and frequency response. The gain was measured at a fixed bias voltage for a heat sink temperature of 83, 103, and 122 degrees Farenheit. The experimental results are plotted in Figure 8. The curve at 86°F represents the response when no external heating is applied to the heat sink. As the temperature increases, the gain increases at the lower frequencies, while it almost decreases linearly at the high end of the band. As the temperature of the diode increases, significant changes are produced in its characteristics. The number of carriers increases due to a lowering of the band gap energy and increased thermal agitation of the electrons. This changes the external impedance of the diode. The mismatch with the transformer may also increase. This explains part of the decrease of the gain at the high end of the band.

2.4 DIODE CHARACTERIZATION

A computer program was written to simulate the behavior of the amplifier. A suitable equivalent network for the diode needed to be derived. As said in Chapter I, using equations (1-1) through (1-5) it is possible in principle to derive an equivalent network for the semiconductor chip by taking into account the proper boundary conditions imposed by the external microwave circuit. Such an approach is not very illuminating because of the complexity of the mathematics and the many simplifying assumptions needed to arrive at tractable results.

Starting from experimental measurements one can derive the equivalent circuit of the diode. This approach will show what effects the variations of several parameters (voltage, temperature, input power) have on the diode. To do this one needs to know the gain and phase response of the amplifier. The gain is given by the magnitude of the reflection coefficient, $|\Gamma|$. The phase can be measured by choosing a suitable reference point in the circuit. The measurement procedure is described in Appendix 7.1. A short circuit at the input of the amplifier was chosen as the reference plane for the phase measurements.

Let Z_c be the characteristic impedance of the output waveguide, Z the input impedance of the amplifier; then the reflection coefficient at the input of the amplifier is

$$\Gamma = \frac{Z - Z_c}{Z + Z_c} \tag{2-1}$$

Knowing $|\Gamma|$ and arg $(\Gamma) = \psi$, the input impedance as shown in Appendix 7.2 is:

$$Z(\omega) = R(\omega) + jX(\omega) \tag{2-2}$$

where

$$R(\omega) = Z_c \frac{1 - |\Gamma|^2}{1 + |\Gamma|^2 - 2|\Gamma|\cos\psi} \tag{2-3}$$

$$X(\omega) = 2Z_c \frac{|\Gamma|\sin\psi}{1 + |\Gamma|^2 - 2|\Gamma|\cos\psi} \tag{2-4}$$

Using equations (2-3) and (2-4), the equivalent circuit of Figure 4-a, and the procedure of Appendix 6.3, the diode equivalent circuit can be calculated from experimental data.

2.4.1 Diode Impedance Dependence on Bias Voltage

The magnitude and the phase of the reflection coefficient were measured for three bias voltages at a fixed tuning short circuit position of 0.2415 inches on a single diode over the entire X-band.

The series negative resistance of the diode is shown in Figure 9. At 6.5V, the negative resistance is flat at -30Ω over a 1GHz bandwidth, while at 7.0V it is constant at -42Ω over a 1.2GHz frequency range. The magnitude of the negative resistance increases with increasing voltage.

The equivalent series capacitance is shown in Figure 10. The great variation of the capacitance with frequency can be explained in part by errors in the phase measurement. The experimental error was found to be ±20°. Also the model of the transformer used in the calculations did not have a VSWR characteristic that agreed with the experimental values of VSWR. Moreover, the equivalent circuit of Figure 4-b does not represent accurately the field configuration around the diode. At a very close distance to the diode, a pure TE_{10} mode does not exist; rather, the prevalent mode is a radial TEM mode. At distances of the order of a guide wavelength from the diode, the radial mode has been

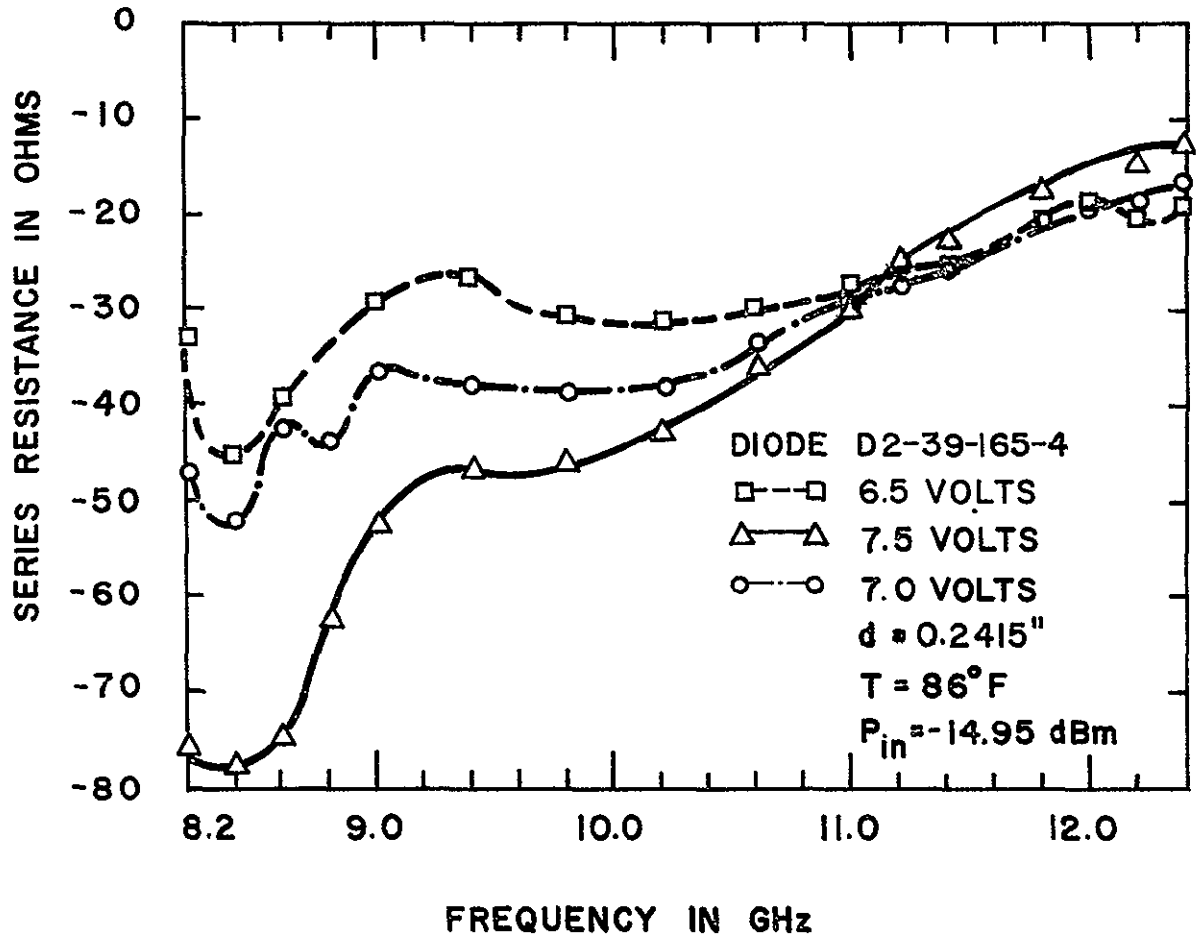

Figure 9. Equivalent Series Resistance of Gunn Diode Versus Voltage

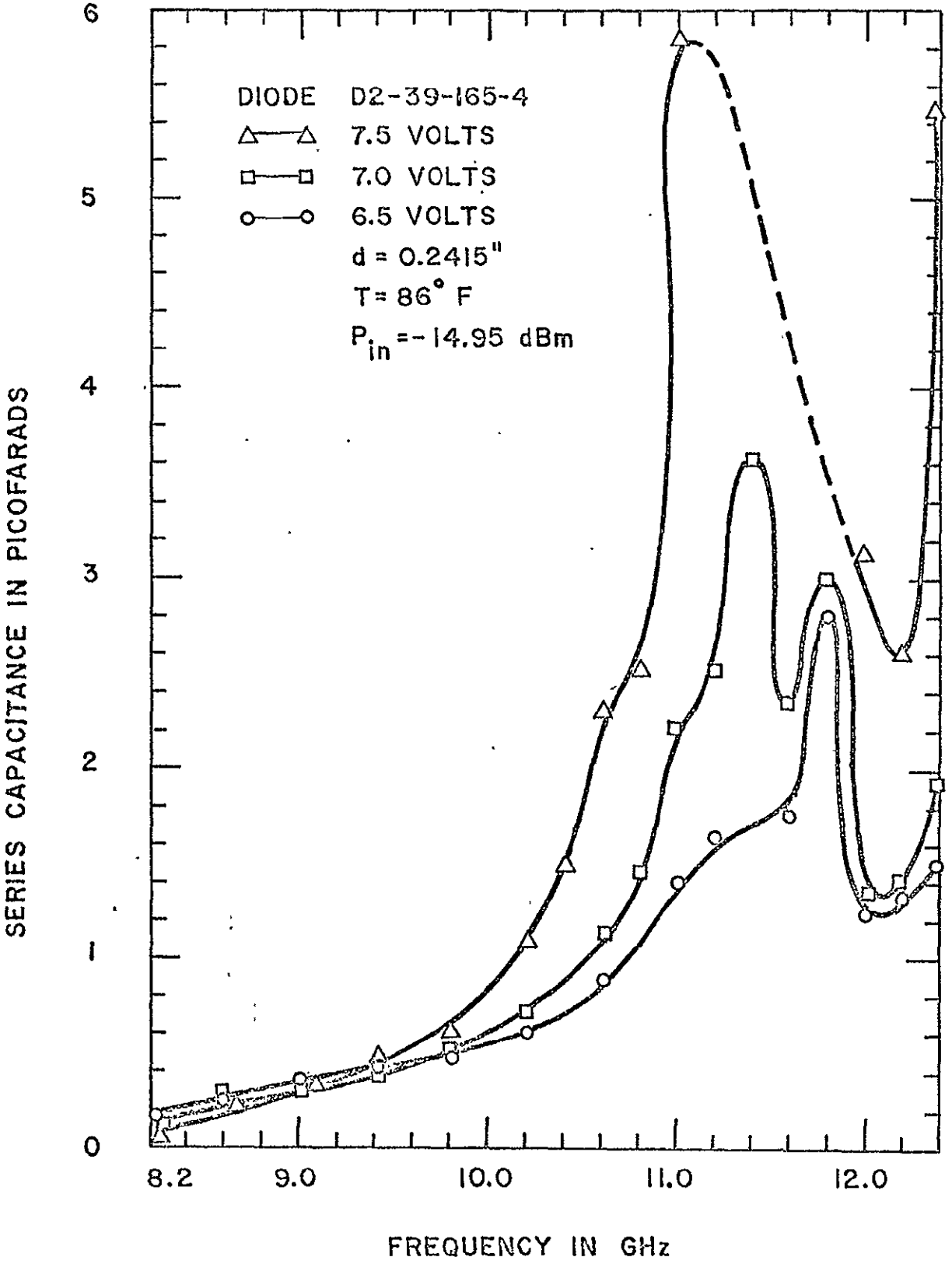

Figure 10. Equivalent Series Capacitance of Gunn Diode Versus Voltage

transformed into a TE_{10} mode. Thus this transformation from a TEM to a TE_{10} mode must be taken into account. It can be modeled by a two port T network (35).

In Figure 10, the capacitance increases to over 1.2pF at the high end of the band. At 6.5V, the peak capacitance is 2.802pF at 11.8GHz, while it peaks at 3.612pF at 11.4GHz for a 7V bias. The curve for 7.5V showed some inductive reactance as indicated by the dashed line. This is probably due to experimental uncertainties and to the incompleteness of the microwave circuit model used to calculate the diode impedance.

2.4.2 Diode Impedance Versus Temperature

The dependance of the series negative resistance and capacitance of the diode on temperature is shown in Figures 11 and 12 for a bias voltage of 7.5V. The temperatures shown are that of the heat sink on which the diode is mounted.

The series resistance at 122°F and 103°F is not much different from the results obtained at room temperature, 86°F. However, at the low end of the band the magnitude of the resistance increases slightly. In terms of frequency response this means an increase in gain if the load seen by the diode does not change drastically due to thermal expansion in the waveguide circuit. At the high end of the band, the magnitude of the resistance decreases with temperature resulting in a lower gain. This then explains the temperature

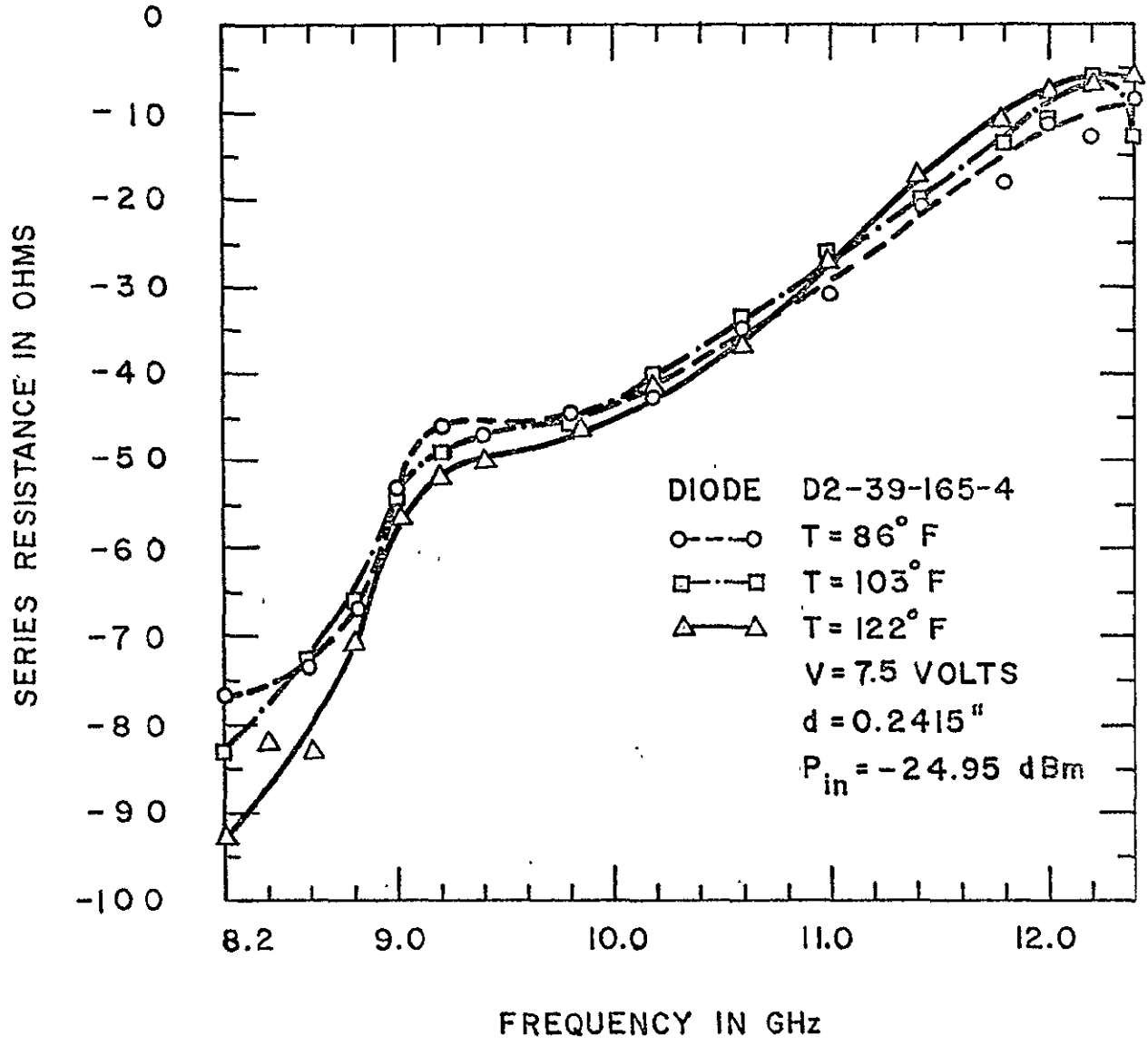

Figure 11. Equivalent Series Resistance of Gunn Diode Versus Temperature

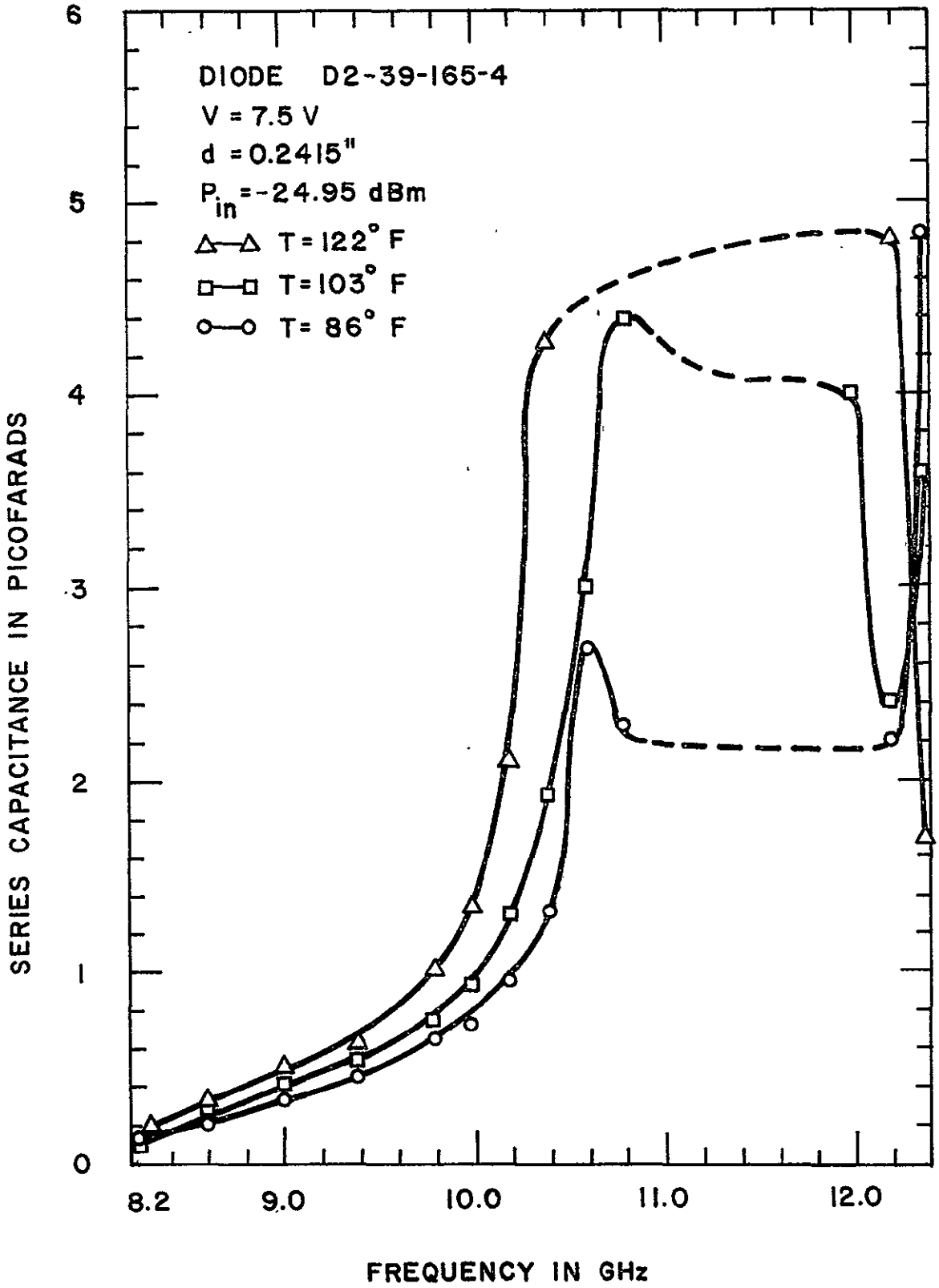

Figure 12. Equivalent Series Capacitance of Gunn Diode Versus Temperature

dependance of the gain shown in Figure 8. Figure 12 shows that the magnitude of the series capacitance increases with temperature. If the diode impedance is represented as a parallel R-C shunt circuit, it will be found that the magnitude of the shunt resistance, R_s, decreases with temperature. This corresponds to an increasing gain as can be shown. Assume a reactanceless situation of a negative resistance, $-R_s$, in shunt with a load resistance R_L. The gain is given by the reflection coefficient:

$$\Gamma = \frac{R_s + R_L}{R_s - R_L} \tag{2-5}$$

If $R_L < R_s$, $|\Gamma| > 1$, then

$$\frac{d|\Gamma|}{dR_s} = -\frac{2R_L}{(R_s - R_L)^2} \tag{2-6}$$

Thus if the shunt negative resistance decreases in magnitude there will be a corresponding increase in gain. The decrease of the equivalent shunt negative resistance with temperature indicates that the diode will enter into oscillation at high temperature. This was experimentally observed when the heat sink temperature was 150°F.

The changes of the diode impedance with temperature suggest that the v-E curve changes with temperature. The dashed line on Figure 12 indicates some inductive reactance.

2.4.3 Diode Impedance Versus Input Power

The impedance of the Gunn amplifier was measured as a function of input power. The diode was biased at 7.5 volts and the input power varied in steps of 5dB from -24.95dBm to -14.95dBm. A plot of the series or shunt negative resistance did not show conclusively any significant variation. However, a plot of the series capacitance shows some variation at high frequencies. This is shown in Figure 13. From 8.2 to 10GHz there is no change of the capacitance with the input drive. From 10.0 to 12.4GHz the series capacitance shows some dependence on input power. From 11 to 12GHz the calculated data shows an inductive reactance. This is probably due to errors in measuring the phase of the reflection coefficient. When the diode is overdriven to saturation, the gain decreases, which indicates that the series negative resistance decreases in magnitude with input signal power.

2.5 OTHER MICROWAVE CIRCUIT

The stepped-impedance transformer is not the only possible circuit that can be used to build waveguide negative resistance amplifiers. Another low to high impedance transformer which was used is the linear taper terminated with a movable short-circuit plane. Unfortunately, the properties of this circuit were not extensively investigated. However, it was possible to obtain amplification with this circuit. A schematic of the circuit is shown in Figure 14.

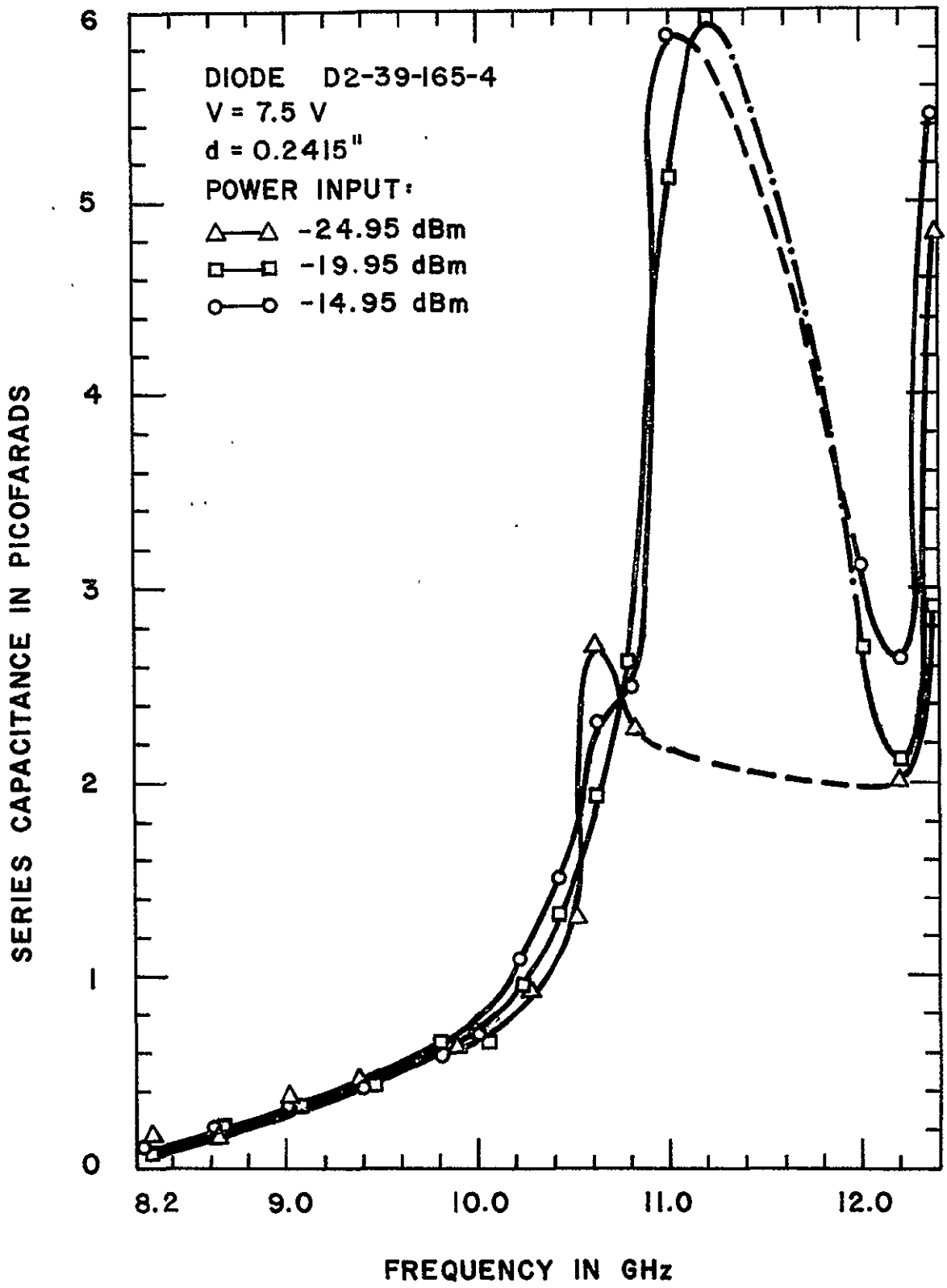

Figure 13. Equivalent Series Capacitance of Gunn Diode Versus Input Signal Power

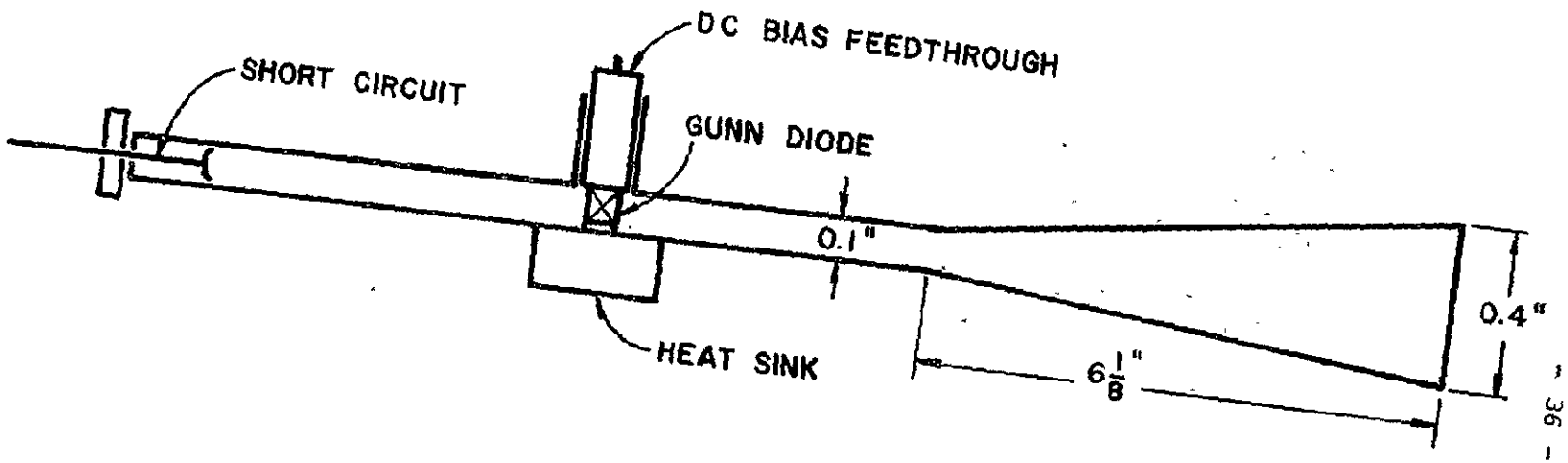

Figure 14. Taper Mount Diagram

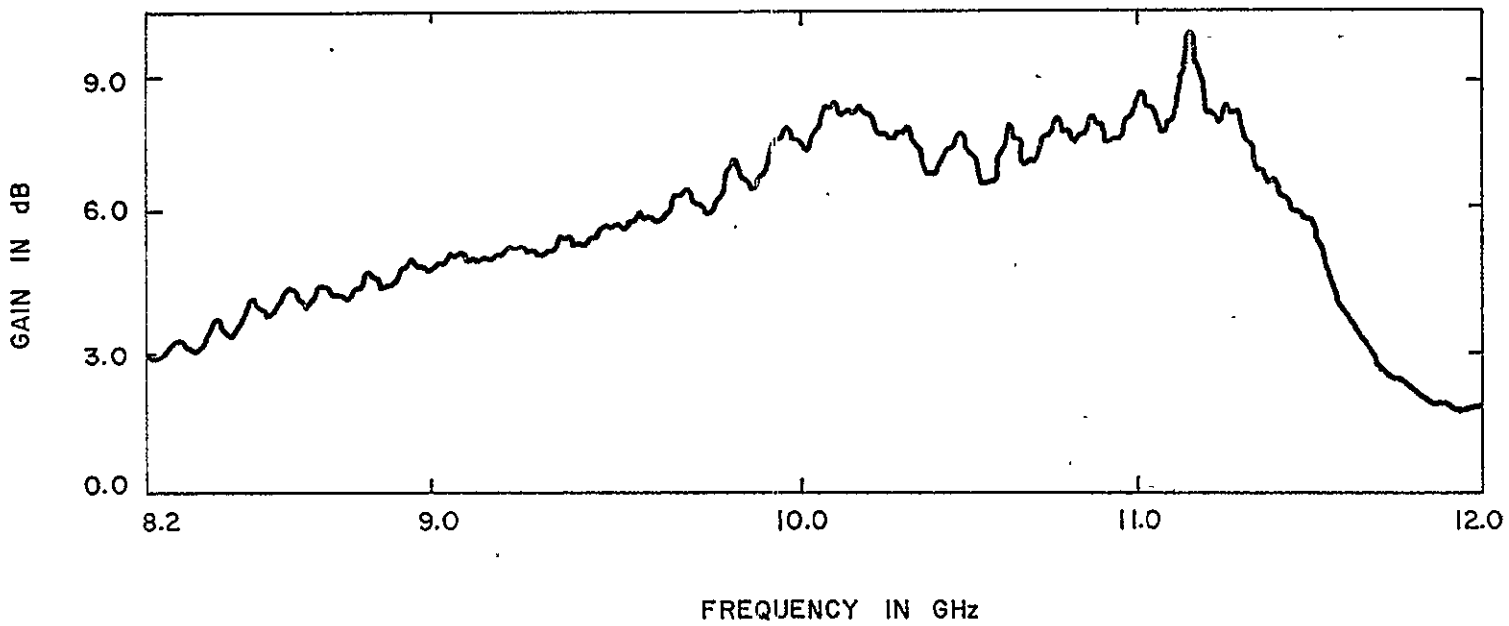

Figure 15. Frequency Response of Diode 82-A5-36 in Taper Mount

The linear taper transformer section reduces the standard waveguide height (0.4 inches) to 0.1 inch, thus producing a 4:1 impedance ratio. The diode is placed in the reduced height section which is terminated by a short circuit.

The frequency response obtained with this circuit is shown in Figure 15 for the diode 82-A5-36 biased at 9 volts. The peak gain is about 9dB. The gain is almost flat at 8dB from 10 to 11.2GHz. The high frequency gain drops very sharply compared to the slow rise of the gain on the low frequency side. For comparison purposes, the same diode was used at the same bias voltage in the stepped transformer circuit. The gain response observed is shown in Figure 6. The midband gain is about 10dB. The taper transformer gives a much sharper cutoff than the stepped impedance transformer.

3. THEORETICAL CONSIDERATIONS

3.1 INTRODUCTION

The results of the preceding chapter are used herein to predict the wideband performance of the amplifier. Some consideration is given to the limitations of optimum negative resistance amplifiers. It is found that the use of a reciprocal coupling network (e.g., directional coupler) gives a gain 6dB below that of the ideal optimum nonreciprocal coupling network (lossless circulator). The use of narrowband filters to shape the frequency response is described.

3.2 COMPUTER SIMULATION

Using the equivalent circuit of Figure 4-b, the gain of the amplifier was calculated theoretically.

Stability considerations lead to the calculation of the load impedance seen by the diode. The diode is considered to be a negative resistance (-R) in shunt with a capacitor, C. The admittance of the diode is

$$Y_D = -\frac{1}{R} + j\omega C \qquad (3\text{-}1)$$

Let the admittance of the load be $Y_L = G_L + jB_L$; then the circuit will oscillate if:

$$Y_L + Y_D = 0$$

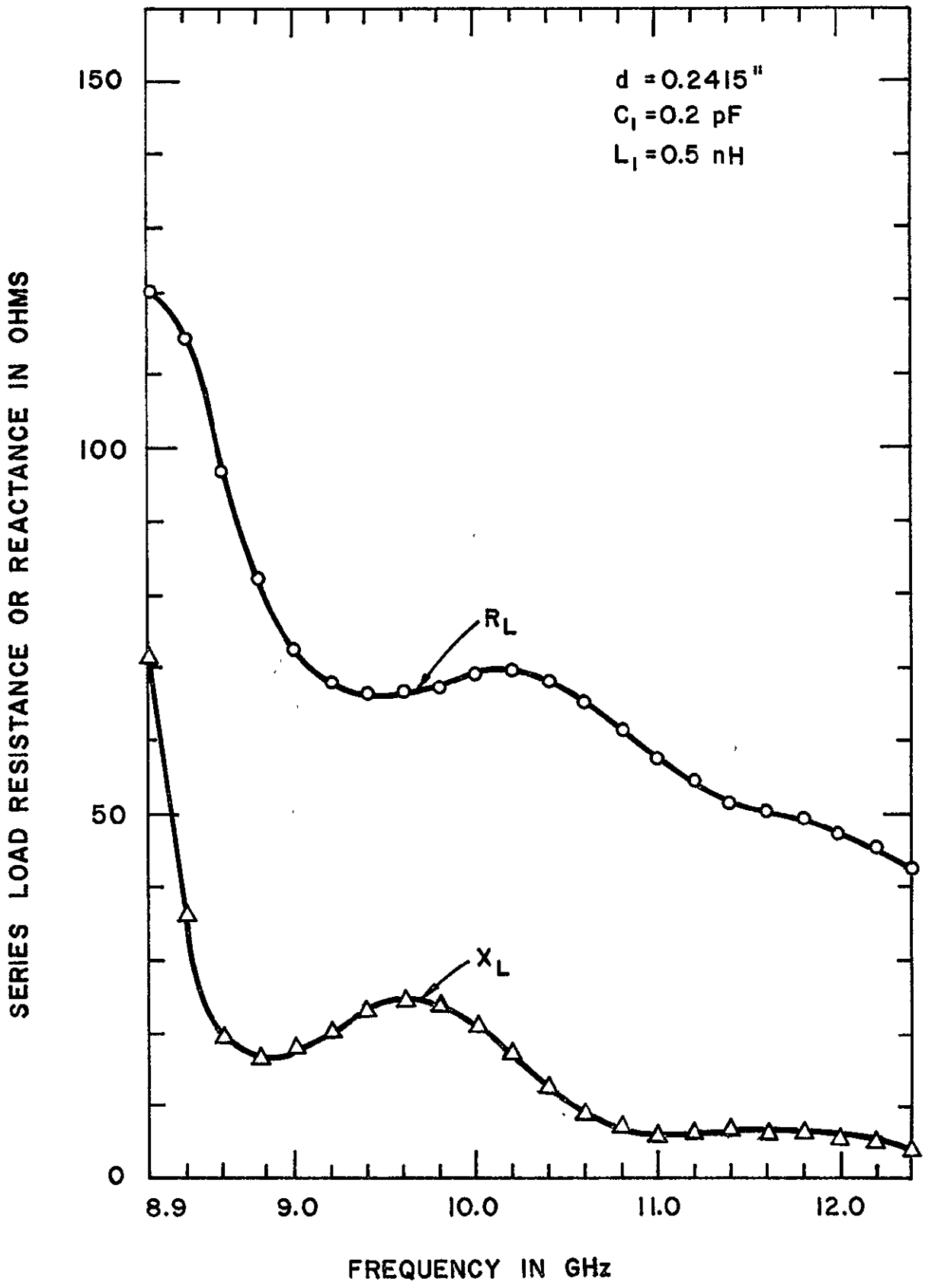

Figure 16. Series Load Resistance or Reactance on the Diode

or

$$G_L + jB_L - \frac{1}{R} + j\omega C = 0 \qquad (3\text{-}2)$$

or

$$G_L = \frac{1}{R}$$

$$B_L = -\omega C$$

Thus if the shunt load conductance is greater than that of the diode and the circuit is not resonant at the terminals of the diode, the amplifier will be stable.

A more appropriate representation of the active device is a series R-C. The series load seen by the diode is shown in Figure 16. The short circuit is placed at 0.2415 inches from the plane of the diode, the experimental value. The series load resistance decreases with frequency, but the rate of decrease is less than that of the magnitude of the series negative resistance calculated in Chapter 2.

3.2.1 Comparison of Experimental and Theoretical Calculations

In the preceding chapter, it was shown that the Gunn diode amplifier can be modeled as a series negative resistance and a capacitance, both of which are frequency dependent. Figure 9 shows that at 6.5V bias, the series negative resistance is flat at about -30Ω over a 1GHz bandwidth. Using this value and a series capacitance of 0.5pF with a

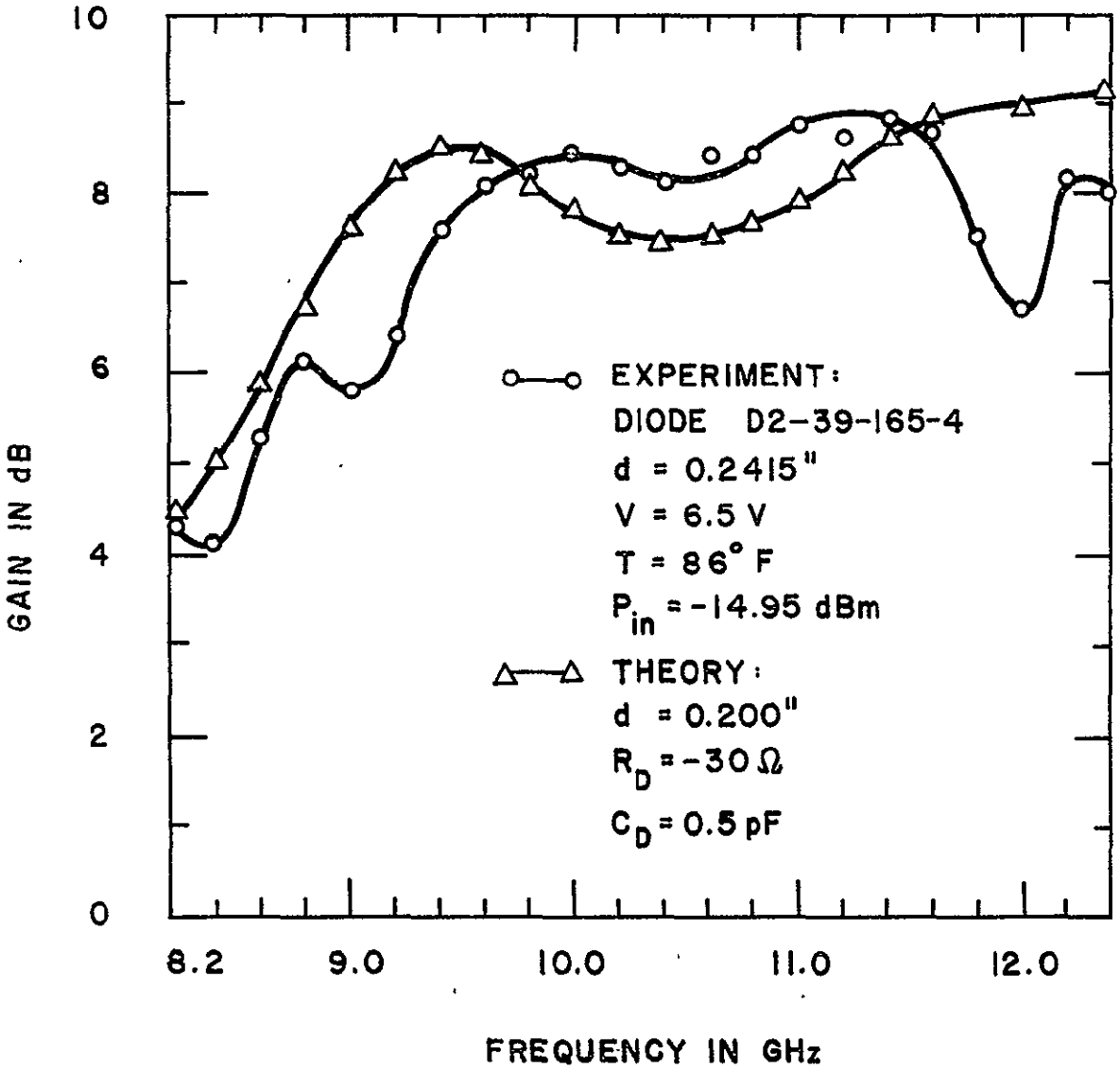

Figure 17. Comparison of Theoretical and Experimental Gain Response

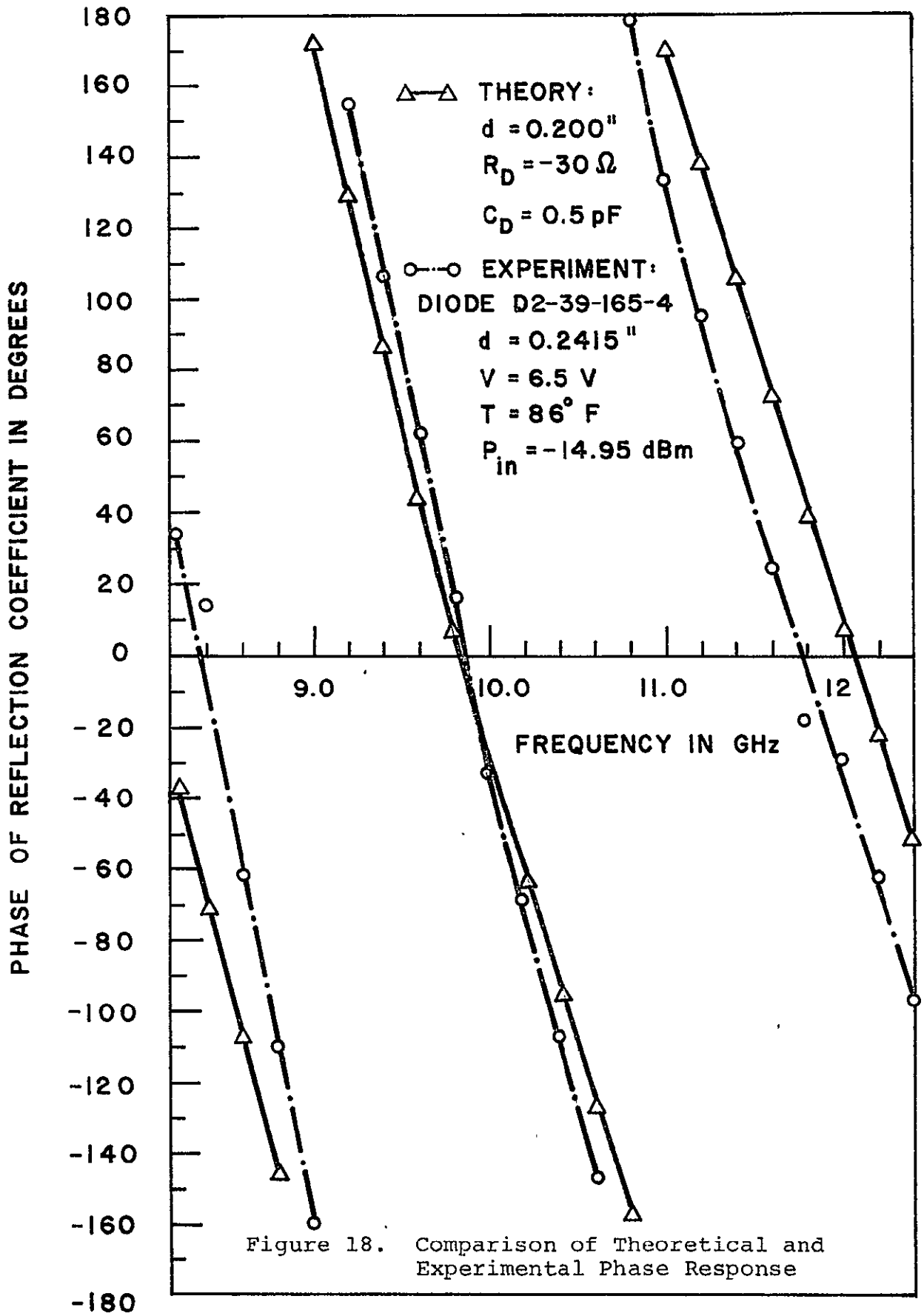

Figure 18. Comparison of Theoretical and Experimental Phase Response

tuning short at 0.200 inches, the frequency response of the amplifier was simulated. The resulting gain characteristic is shown in Figure 17. The experimental points at 6.5V are also shown. There is excellent agreement between theoretical calculations and experiment. The largest deviation between the two curves is less than 3dB. The midband gain is about 8dB.

The phase of the reflection coefficient was also calculated for the same constant negative resistance and capacitance. A comparison of experiment and theory is shown in Figure 18. At midband, the two phase characteristics are almost identical. Both sets of data indicate a nonlinear phase characteristic. At both ends of the band there is a substantial deviation between theory and experiment, probably due to the constant capacitance assumption.

3.2.2 Tuning of the Frequency Response

Using the same model of the diode as in the preceding section, the gain and phase response of the amplifier were calculated theoretically for five positions of the tuning short circuit ranging from 0.1 inches to 0.5 inches. The gain is shown in Figure 19. As the amplifier is tuned, the peak gain moves down in frequency. When the short circuit is at 0.2 inches, which is close to the experimental value, the peak gain is at 8dB. Such a tuning of the frequency response has been observed experimentally. The calculated phase response for several values of the short circuit

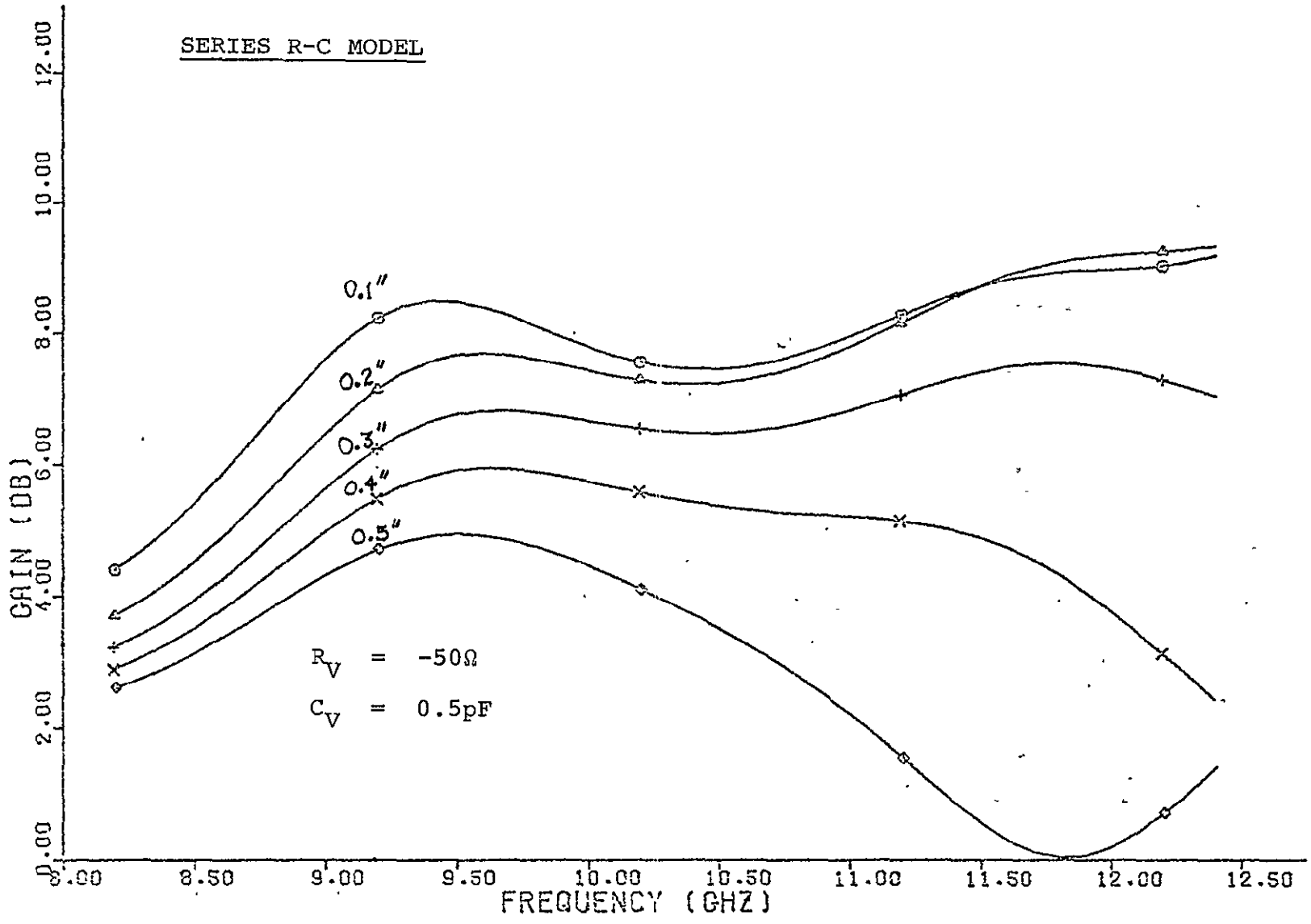

Figure 19. Gain Response Versus Tuning Short Position

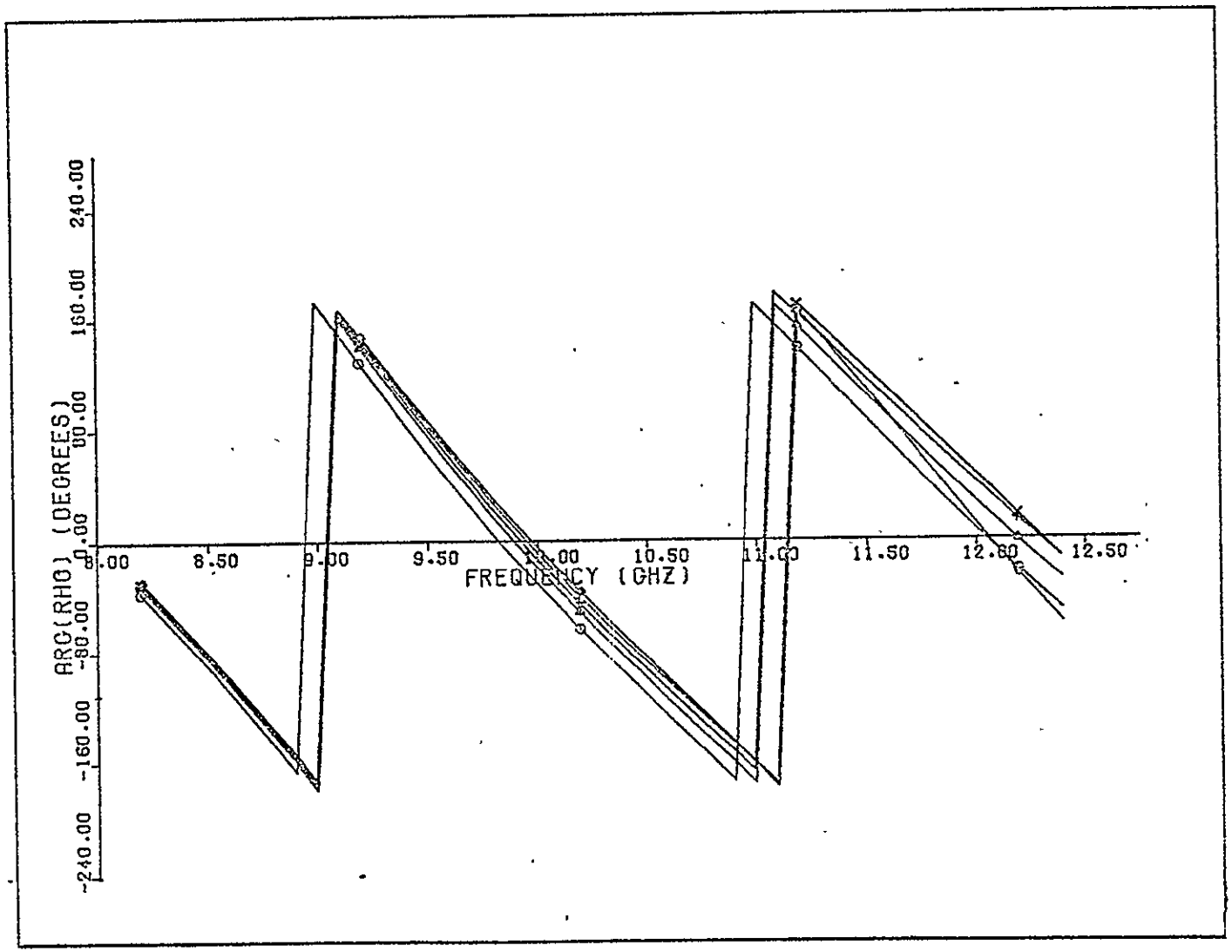

Figure 20. Phase Response Versus Tuning Short Position

position is shown in Figure 20. Note the nonlinearity, which is reminiscent of the experimental measurement.

This simulation indicates that with a crude model of the amplifier, the gain response can be predicted. In systems applications, the performance can be optimized by a judicious choice of the diode parameters and the circuit elements.

3.3 BROADBAND NEGATIVE RESISTANCE AMPLIFIERS

For some applications it may be necessary to design Gunn Effect amplifiers having flat gain characteristics over a wide range of frequencies. Since the diode can be represented as a negative resistance in parallel with a capacitor, the broadbanding problem is then reduced to the design of an optimum coupling network having specified characteristics over a certain range of frequencies. What is the best performance that can be achieved with such optimum coupling networks? That is the topic of the next section.

3.3.1 Limitations on Optimum Negative Resistance Amplifiers

There are physical limitations on the broadband impedance matching of any load (36, 37). The works of Fano and Youla (38) show that there is a tradeoff between the gain of a reflection type amplifier and its bandwidth.

Consider the network of Figure 21, where a passive load R_0 - C is to be matched to a resistance R_L by a lossless coupling network. The input impedance at the terminals of

the load is Z_1. The impedance seen by R_L is Z_2. The reflection coefficient at the terminals of R_L is (37):

$$\Gamma = \frac{R_L - Z_2^*}{R_L + Z_2} \tag{3-3}$$

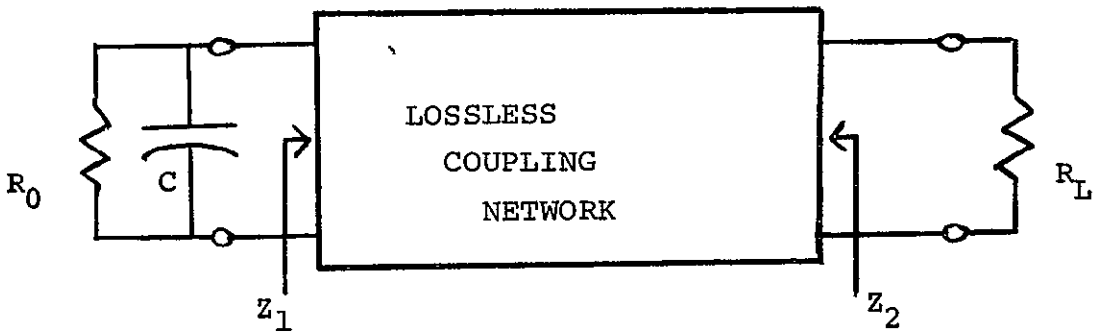

Figure 21. Impedance Matching Problem

where Z_2^* is the complex conjugate of Z_2. Bode (37) has shown that the smallest value of $|\Gamma|$ is given by the equation,

$$\int_0^\infty \ln \frac{1}{|\Gamma|}\, d\omega \geq \frac{\pi}{R_0 C} \tag{3-4}$$

If we assume over a certain range of frequencies that

$$|\Gamma| = \begin{cases} \text{constant } k & \text{for } \omega_1 \leq \omega \leq \omega_2 \\ 1 & \text{otherwise} \end{cases} \tag{3-5}$$

then the optimum result is given by

$$\int_{\omega_1}^{\omega_2} \ln \frac{1}{|\Gamma|}\, d\omega = \frac{\pi}{R_0 C} \tag{3-6}$$

from which

$$|\Gamma| = e^{-\frac{\pi}{R_0 C(\omega_2 - \omega_1)}} \qquad \omega_1 < \omega < \omega_2 \tag{3-7}$$

Equation (3-7) is shown in Figure 22-a when R_0 is positive.

If the resistance R_0 is replaced by a negative resistance, we may have a reflection type amplifier. Youla and Smilen (38) have shown that the gain for a circulator coupled negative resistance amplifier is limited as follows:

$$\int_0^\infty \ln G_T \, d\omega \leq \frac{2\pi}{RC} \tag{3-8}$$

Assuming constant gain from ω_1 to ω_2 and zero gain outside this band, then the maximum gain is

$$\int_{\omega_1}^{\omega_2} \ln G_T \, d\omega = \frac{2\pi}{RC} \tag{3-9}$$

or

$$G_T = e^{\frac{2\pi}{RC(\omega_2-\omega_1)}} \qquad \text{for } \omega_1 \leq \omega \leq \omega_2$$

This equation is shown in Figure 22-b.

For the reciprocally coupled amplifier (directional coupler), the gain is bounded by (38):

$$\int_0^\infty \ln \left[2\sqrt{G_T} - 1\right] d\omega \leq \frac{2\pi}{RC} \tag{3-10}$$

If G_T is constant from ω_1 to ω_2, then the maximum gain is:

$$G_T = \frac{1}{4}\left(1 + e^{\frac{2\pi}{RC(\omega_2-\omega_1)}}\right)^2 \tag{3-11}$$

Since $1 \leq e^{\frac{2\pi}{RC(\omega_2-\omega_1)}}$ then $\frac{1}{4}\left(1 + e^{\frac{2\pi}{RC(\omega_2-\omega_1)}}\right)^2 \leq e^{\frac{2\pi}{RC(\omega_2-\omega_1)}}$.

So the ideal circulator coupled amplifier has a 6dB gain advantage over the reciprocally coupled one.

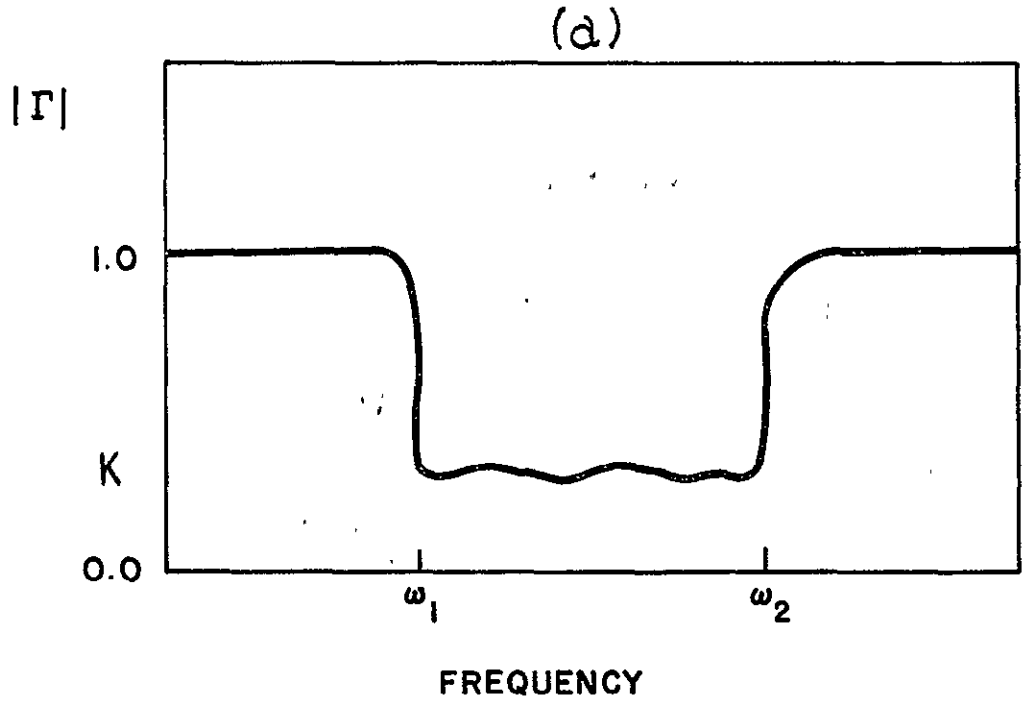

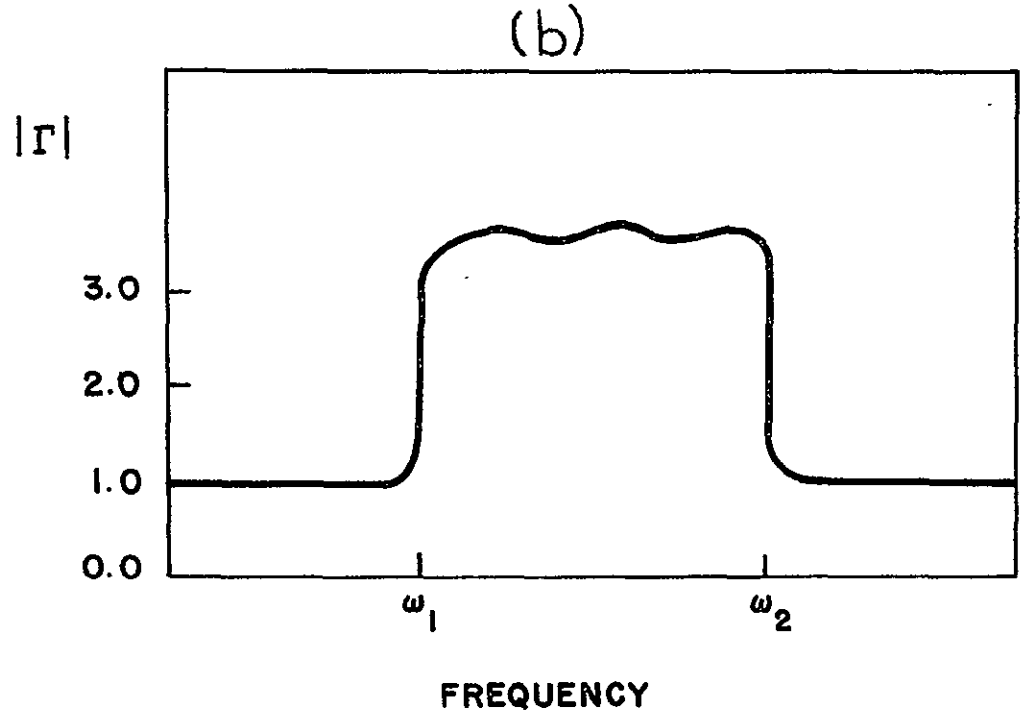

Figure 22. (a) Impedance Matching for a Positive Load
(b) Impedance Matching for a Negative Resistance

3.3.2 Low Pass Optimum Negative Resistance Amplifiers

The ideal rectangular shaped gain response is physically unrealizable, as can be shown from the Paley-Wiener criterion (39). For realizable networks, some approximations are needed.

The maximally flat gain characteristic is given by (38)

$$G_T(\omega^2) = \frac{K_n}{1 + \left(\frac{\omega}{\omega_c}\right)^{2n}} \tag{3-12}$$

Using equation (3-8), the maximum gain limitation is (38):

$$K_n = \left[1 + \frac{\sin\frac{\pi}{2n}}{\pi RCB_c}\right]^{2n} \tag{3-13}$$

where $\omega_c = 2\pi\beta_c$ = cutoff frequency.

The Chebychev characteristic is given by (38):

$$G_T(\omega^2) = \frac{K_n}{1 + \varepsilon^2 T_n^2\left(\frac{\omega}{\omega_c}\right)} \tag{3-14}$$

where $T_n(\frac{\omega}{\omega_c})$ is the nth order Chebychev polynomial and ε is a positive number less than 1. The maximum realizable gain is:

$$K_n = \varepsilon^2 \sinh^2\left[n \sinh^{-1}\left\{\frac{\sin\frac{\pi}{2n}}{\pi RCB_c} + \sinh\left(\frac{1}{n}\sinh^{-1}\frac{1}{\varepsilon}\right)\right\}\right] \tag{3-15}$$

3.3.3 Quarter-Wave Transformer Coupled Amplifiers

A low pass frequency response can be transformed to the bandpass response of a quarter-wave transformer (40), by letting in equations (3-12) and (3-14):

$$\frac{\omega}{\omega_c} = \frac{\cos\theta}{\mu_0} \tag{3-16}$$

where

$$\theta = \frac{\pi}{2} \frac{\lambda_{g0}}{\lambda_g}$$

λ_{g0} = guide wavelength at the center frequency, f_0.

λ_g = guide wavelength at the frequency f.

$\mu_0 = \sin(\frac{\pi}{4} \omega_q)$

ω_q = fractional bandwidth of the transformer.

Thus a quarter-wave transformer, terminated with a constant negative resistance, under stable conditions, will amplify signals.

The maximally flat gain characteristic is given by

$$G_T(\omega^2) = \frac{K_n}{1 + \left(\frac{\cos\theta}{\mu_0}\right)^{2n}} \tag{3-17}$$

and the Chebychev response by:

$$G_T(\omega^2) = \frac{K_n}{1 + \varepsilon^2 T_n^2 (\frac{\cos\theta}{\mu_0})} \tag{3-18}$$

Equations (3-17) and (3-18) were modeled on the computer for a center frequency of 10GHz. The response of the maximally flat case, normalized to the midband gain, is shown in Figure 23. For n = 2, the gain is flat over a 400MHz bandwidth; the 3dB bandwidth is 1.3 GHz. The three section transformer was designed for the same fractional bandwidth, but it gives a flat gain response over a 600MHz

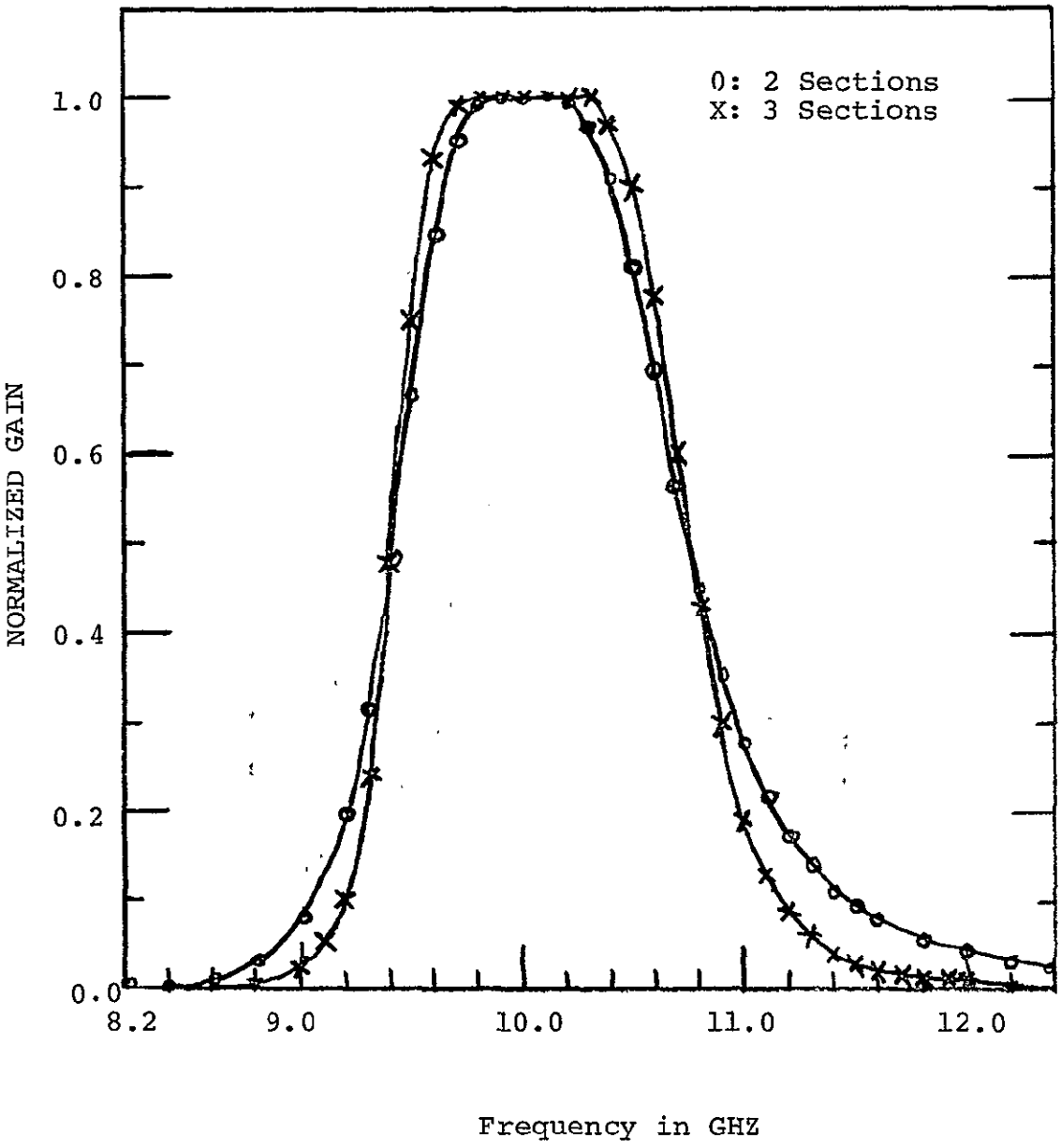

Figure 23. Gain Response of Maximally Flat Quarter Wave Transformer

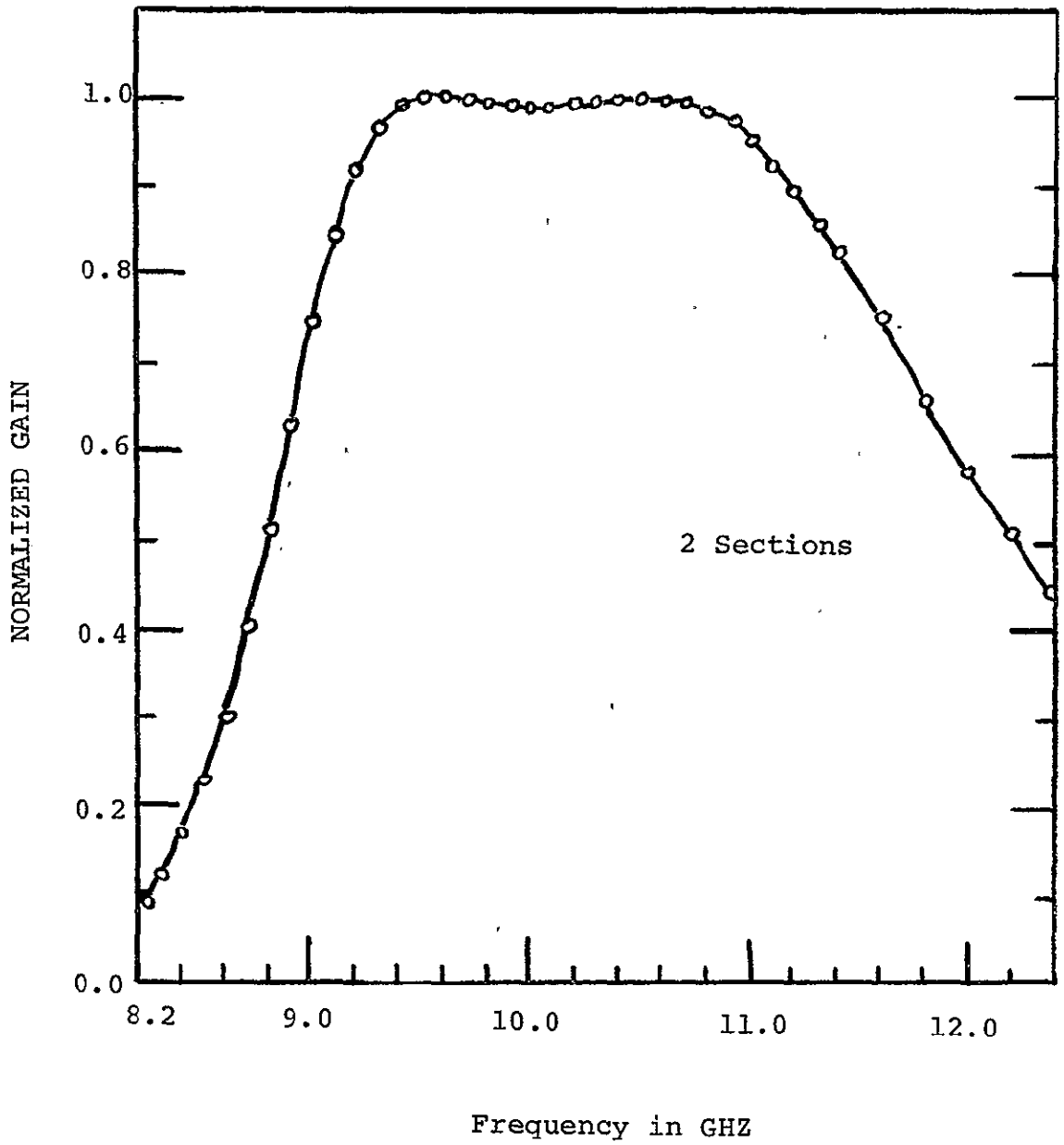

Figure 24. Gain Response of Chebychev Quarter Wave Transformer

bandwidth. As expected the cutoff is much sharper for the three-section transformer. The normalized gain response of the Chebychev amplifier for n = 2, $\varepsilon = 0.1$ and a 10% fractional bandwidth is shown in Figure 24. The computed 3dB bandwidth is 3.4GHz, which exceeds the performance of the three section maximally flat design.

The design of stepped impedance quarter-wave transformers is extensively covered by Matthei et al. (40), and by Gledhill and Issa (41).

3.4 NARROW BAND, DOUBLE TUNED RESPONSE

Garbrecht and Heinlein (42) have shown that by using capacitive screws, a reflection type amplifier can be simply broadbanded. In an experiment, a slide screw tuner was placed in front of the amplifier, and, by adjusting the depth of penetration of the probe and its longitudinal position, the magnitude of the feedback signal to the amplifier can be varied and properly phased to give negative or positive feedback.

The gain of the amplifier could then be equalized over narrow bandwidths.

The results of such an experiment are shown in Figure 25. A doubly tuned response centered at about 9.75GHz is shown. The 3dB bandwidth is 110MHz and the midband gain is 20dB. The penetration of the screw in the guide is 0.1239 inches. By adjusting the slide screw tuner, narrow band (i.e., bandwidth less than 1GHz) maximally flat response can be obtained.

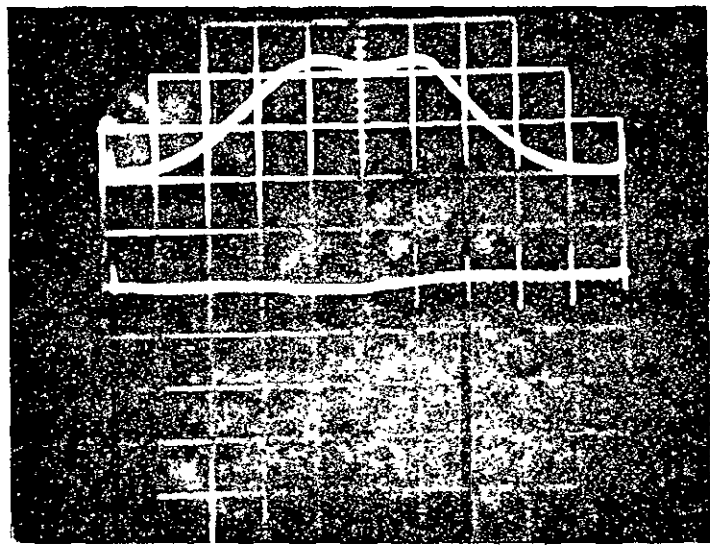

Figure 25. Narrow Band Double Tuned Response

The main problem in this experiment was that the tuner was placed in front of the transformer several guide wavelengths from the diode. In the above experiment, the screw was placed at 11.9 inches from the output flange of the transformer. This increases the frequency dependance of the input impedance of the amplifier. The goal in using the slide screw tuner was to equalize the broadband response of the diode to obtain a flat gain characteristic. However, it is believed that if the tuning screw could be placed closer to the diode, we could have verified the broadbanding procedure described in (42).

4. PERFORMANCE

The performance of the CW waveguide Gunn amplifier will be characterized in terms of power output, dynamic range, AM-to-PM conversion, noise figure and phase linearity.

4.1 POWER OUTPUT

The CW diodes used in the experiments were generally low power devices. Figure 26 shows the power output of a typical diode at four bias voltages and a fixed tuning short circuit position. The variation of power output with bias voltage is similar to the voltage dependance of the gain. At the low edge of the band, the power increases with bias while it decreases at the high end. This corresponds to a shift toward lower frequencies of the peak gain frequency with changes in bias voltage.

The peak power output at 10 volts is 10mW. Since the diode converts DC power to microwave power, one can define the conversion efficiency of the diode. The DC to microwave conversion efficiency is

$$\eta = \frac{P_{out} - P_{in}}{P_{DC}} \qquad (4\text{-}1)$$

where

P_{out} = the microwave output power

P_{in} = the microwave input power

P_{DC} = the DC input power

Typical efficiencies were in the range of three to five per

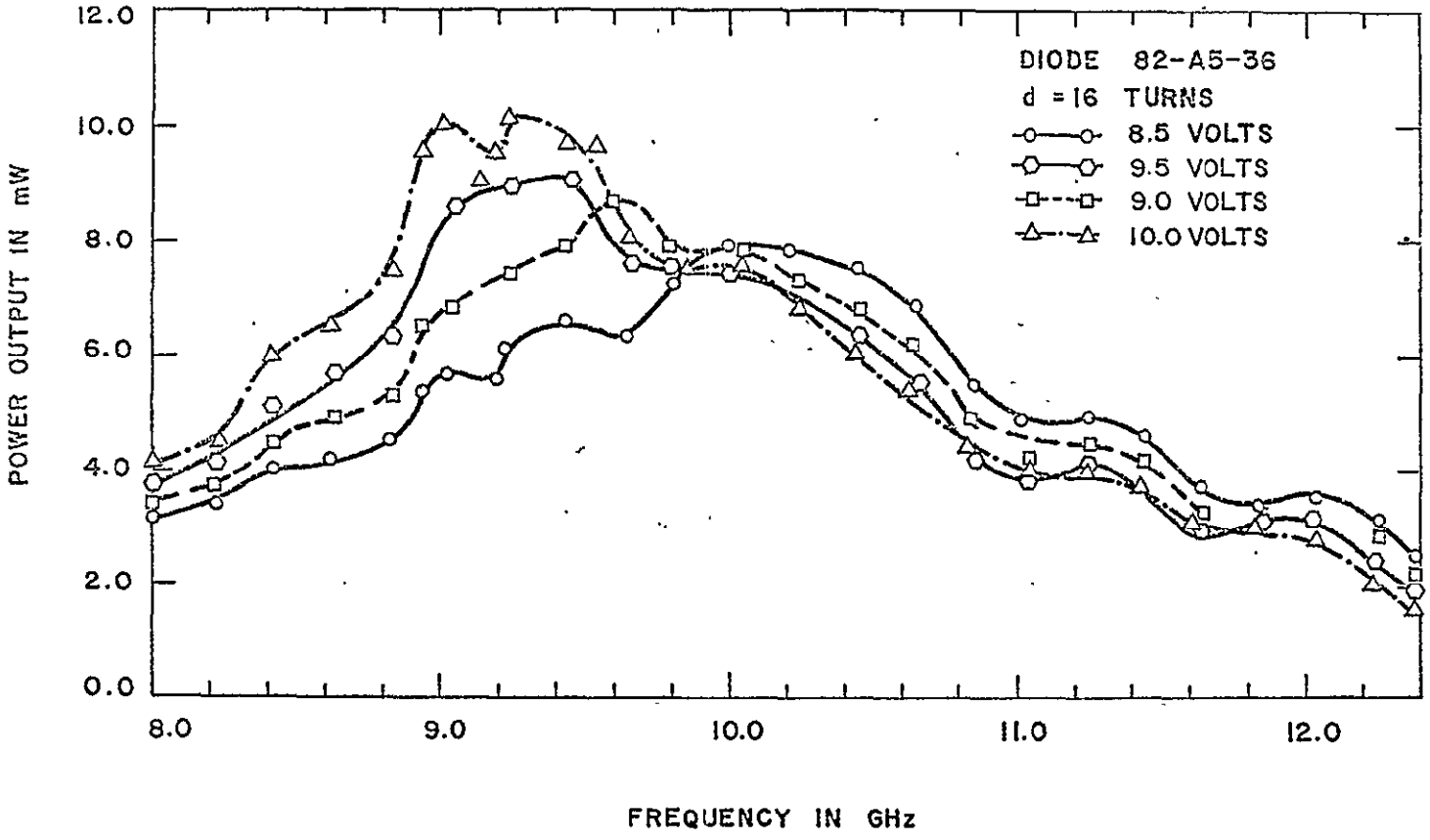

Figure 26. Power Output Versus Voltage

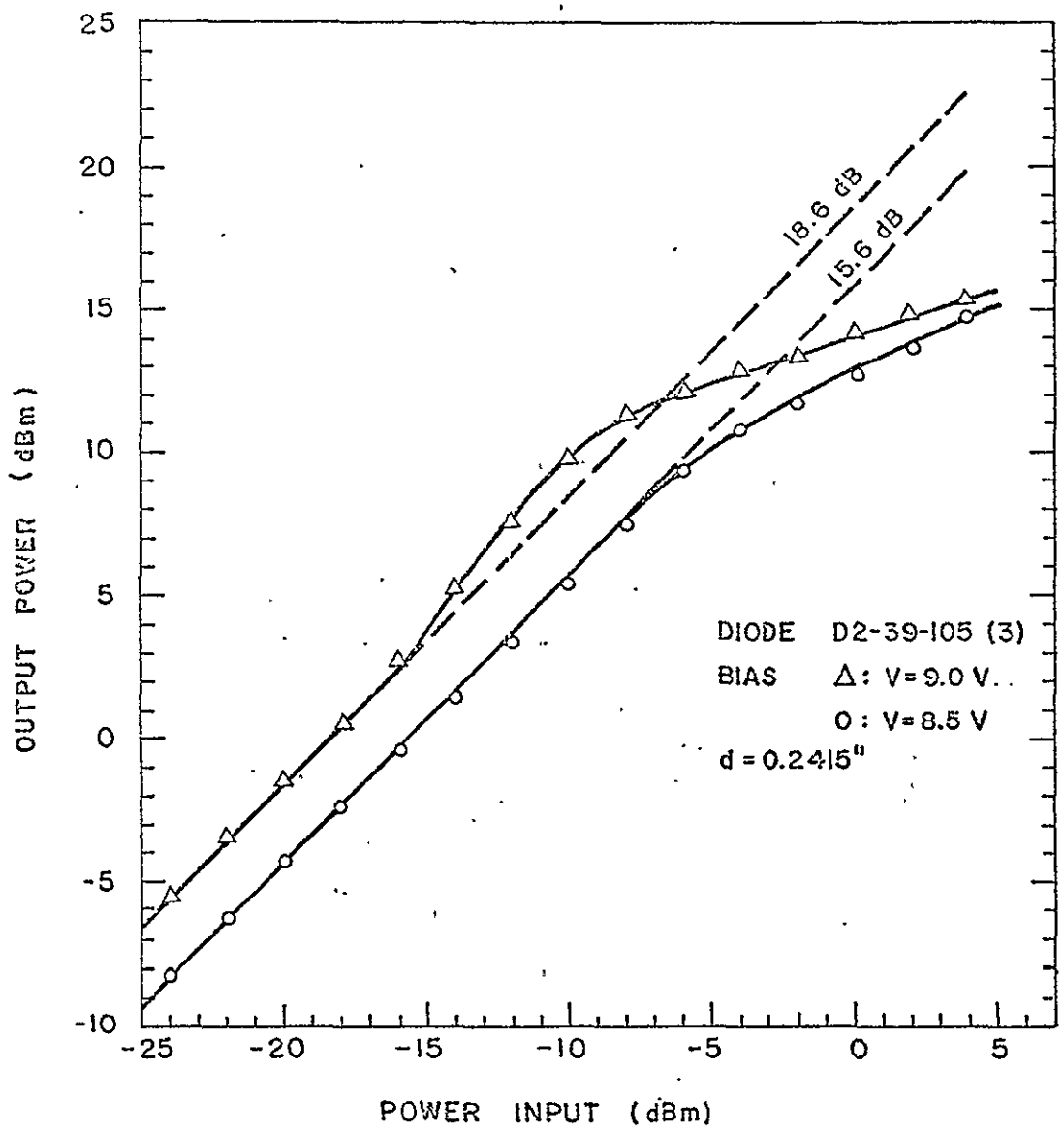

Figure 27. Dynamic Response Versus Voltage

cent. Higher power output can be obtained by using more efficient diodes and a better coupling network to minimize reflections in the output transmission line.

4.2 DYNAMIC RANGE

The CW Gunn amplifier has an extremely wide linear dynamic range. A 94dB linear range was measured. The variation of the linear range with bias voltage is shown in Figure 27 at a fixed short circuit position. At 8.5 volts the linear gain is 15.6dB; gain compression starts at -7dBm input power. At 9 volts the gain is 18.6dB but the linear range is considerably reduced. The gain becomes nonlinear at -15dBm input power. Thus a 0.5 volt increase in bias results in an 8dB loss in dynamic range. As seen in Chapter 2, a bias voltage increase results in an increase in gain. At high gain the amplifier saturates at a low input power. Thus it is seen that the optimum operation of the CW Gunn amplifier depends critically on the bias operating voltage. Very tight regulation of the voltage source is needed to stabilize the characteristics of the amplifier.

4.3 PHASE LINEARITY

The phase response of the amplifier was measured against changes in bias voltage and temperature.

4.3.1 Phase Response Versus Bias Voltage

The phase response of the step transformer amplifier as a function of bias voltage is shown in Figure 28 for three bias values. Below 11GHz for a fixed bias the phase

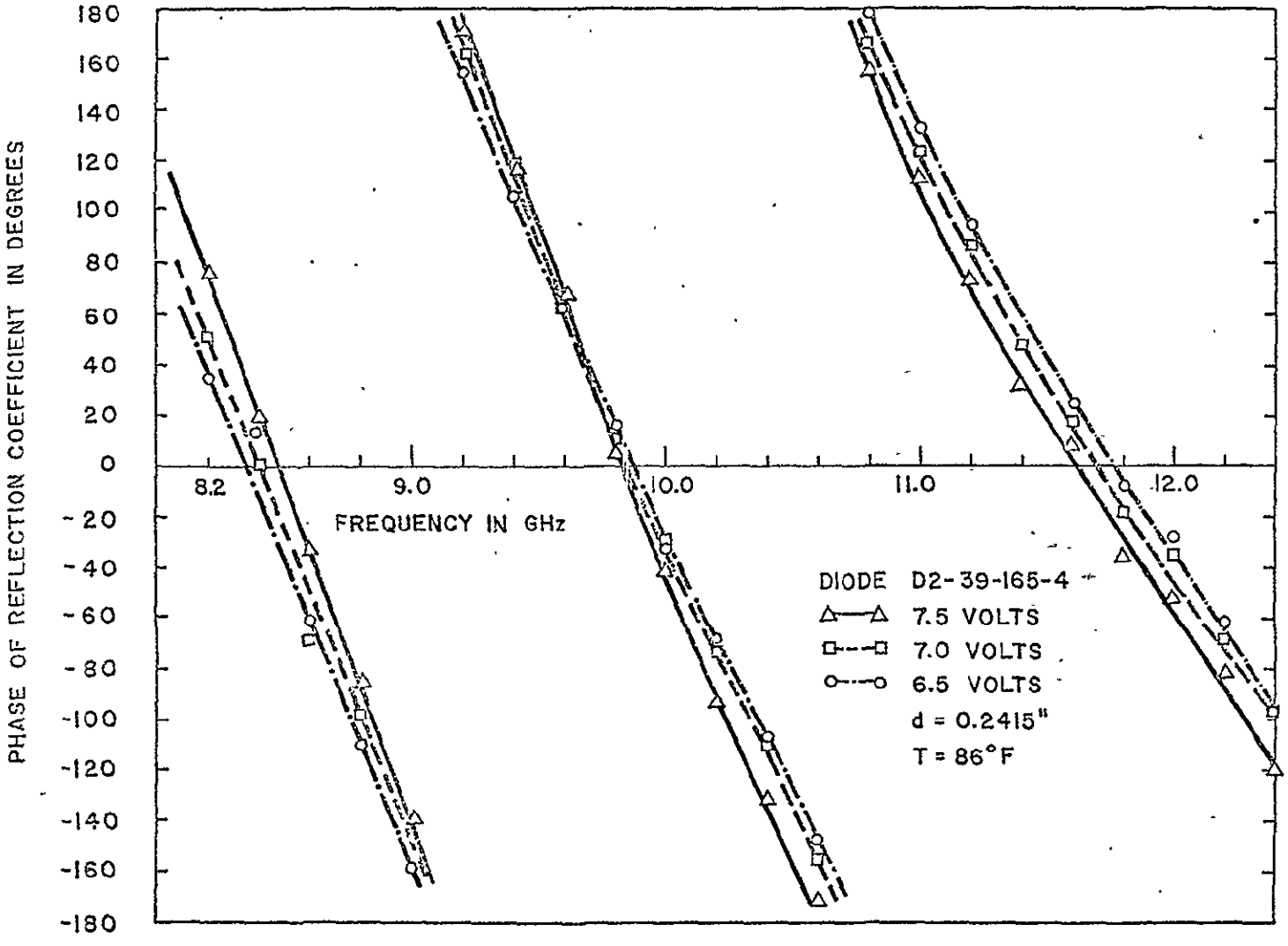

Figure 28. Phase Response Versus Voltage

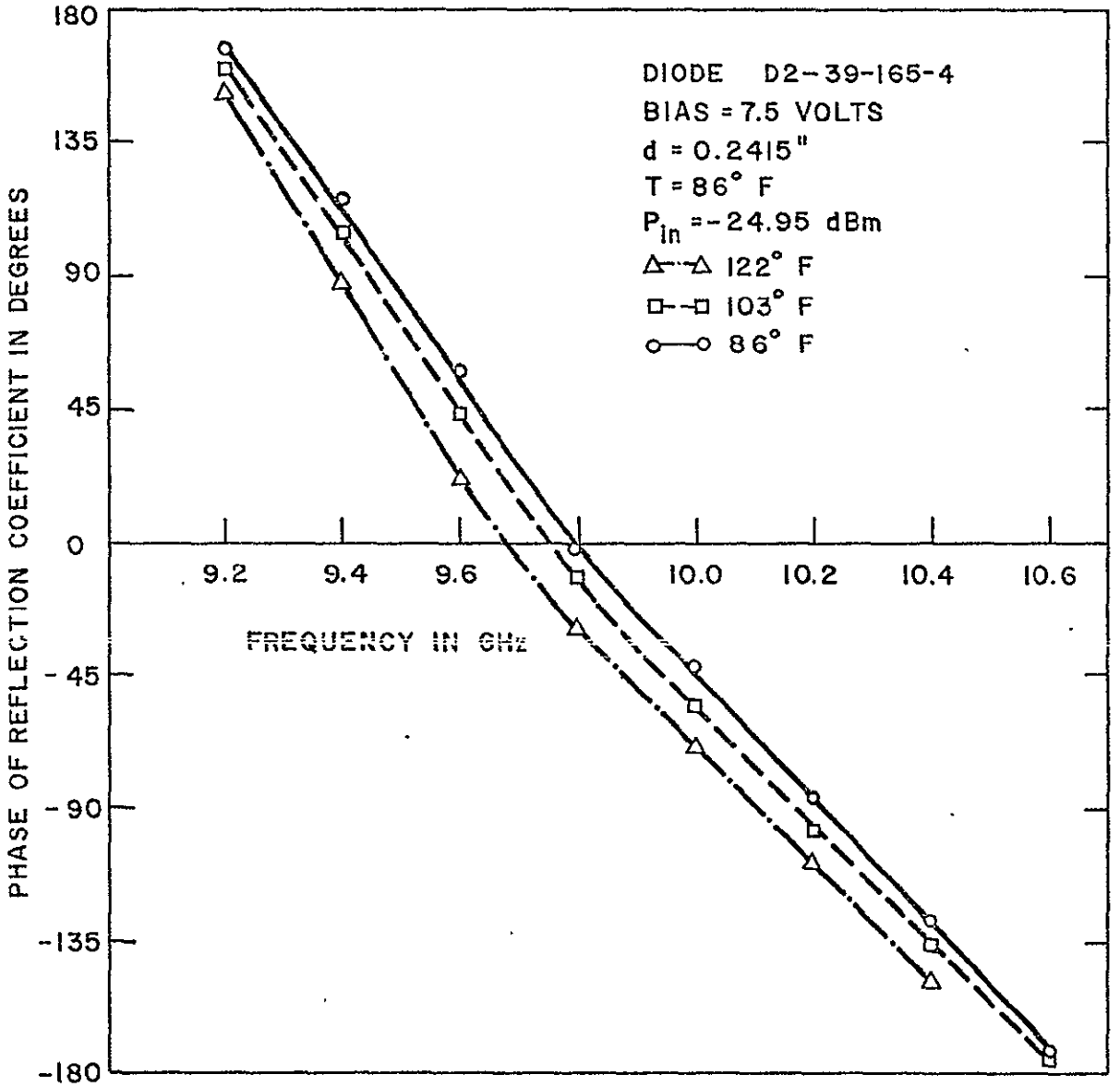

Figure 29. Phase Response Versus Temperature

response is linear within experimental errors. At the high end of the band there is some nonlinearity. The changes in phase response are due to the dependance of the diode impedance on voltage. The reactive part is the cause of the observed changes in phase response.

4.3.2 Phase Versus Temperature

The variation of the phase response of the Gunn effect amplifier as a function of heat sink temperature is shown in Figure 29, at a fixed bias voltage. The phase of the reflection coefficient is seen to decrease with increasing temperature. As shown in Chapter 2, the diode impedance changes with heat sink temperature. The changes of the impedance are mainly due to changes in carrier concentration, the temperature dependance of the mobility and increased diffusion current. This last effect is more prominent in relatively short devices (10 - 11 microns) as used in these experiments (29). At the peak gain frequency, 9.5GHz, the phase decreases from 60° at 86°F to 40° at 103°F and to 20° at 122°F or about a change of 1° per degree increase of the heat sink temperature.

4.4 AM-TO-PM CONVERSION

AM-to-PM conversion in an amplifier refers to the dependence of its phase response on the input power. It is a basically nonlinear effect which is important in broadband amplifiers like traveling wave tubes. In frequency modulated or phase modulated systems, AM-to-PM conversion

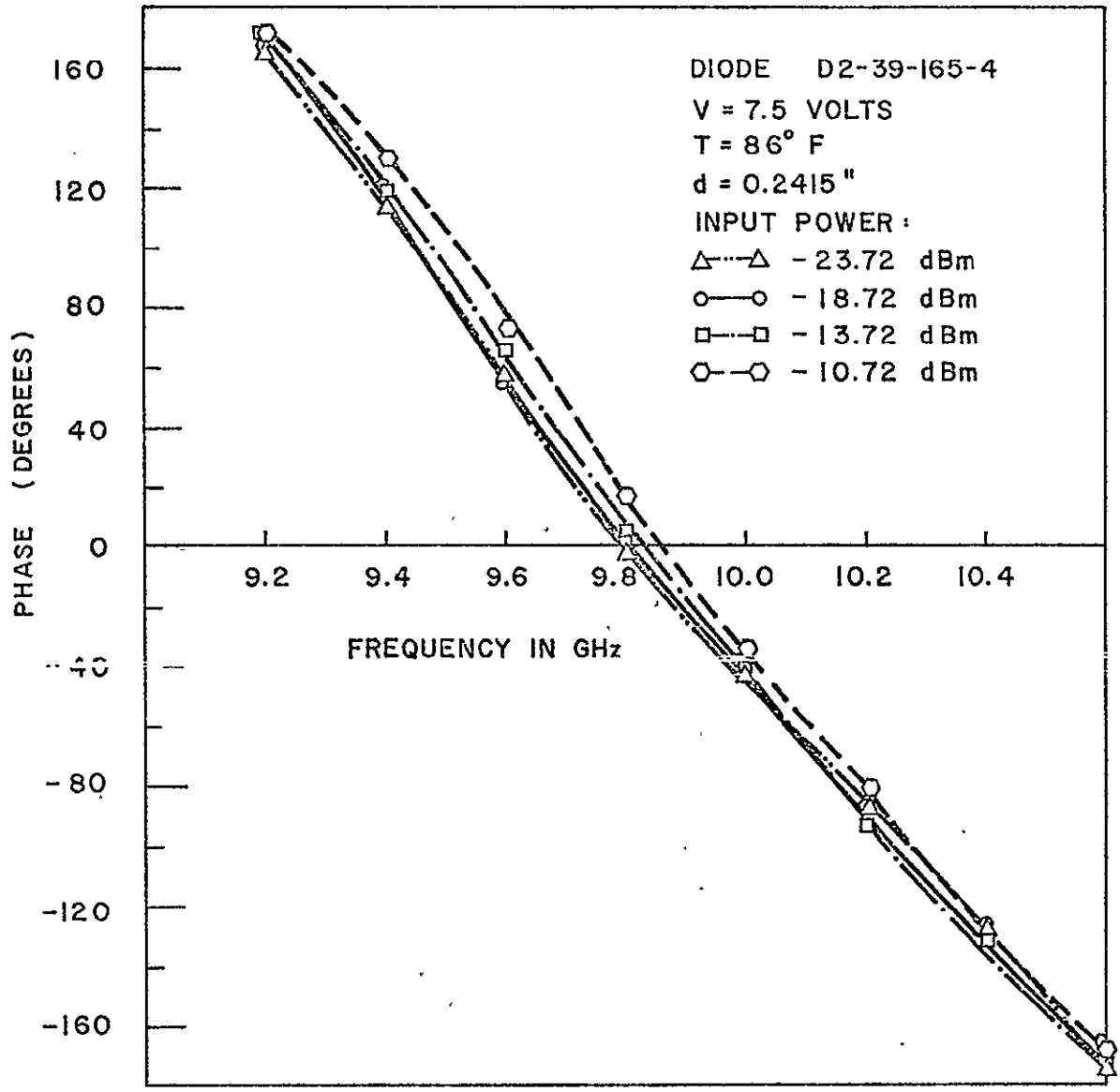

Figure 30. Phase Response Versus Input Signal Power

results in a degradation of the output signal-to-noise ratio of the detector.

The phase response of a Gunn diode amplifier was measured as a function of input power and is shown in Figure 30. The diode was biased at 7.5 volts and the heat sink temperature was 86°F. At power levels below -18.72dBm, there was no measurable change in phase due to input power variation. A 5dB increase of the input power results in a 10° phase at 9.6GHz. A further increase from -13.72dBm to -10.72dBm causes a phase change of about 6°. The relative change of the phase of the reflection coefficient with input drive is not uniform with frequency.

4.5 NOISE PERFORMANCE

The noise model of a Gunn diode amplifier can be represented as shown in Figure 31:

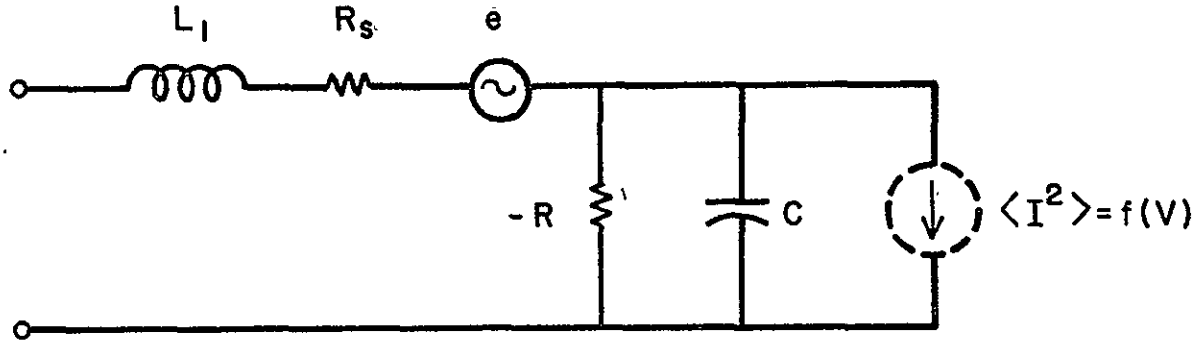

Figure 31. Noise Equivalent Circuit of Gunn Amplifier

The series resistance associated with the diode is a source of white noise. The noise voltage generated by such a

resistor at a temperature T is given by:

$$\langle e^2 \rangle = 4kTR_s B_n \tag{4-2}$$

where k is Boltzmann's constant and B_n is the noise bandwidth of the amplifier.

The diode generated noise is represented by a voltage dependent current source. The power spectral density of the noise output of an amplifier with input termination at a temperature T_0 is given by

$$S_y(\omega) = [F(\omega) - 1]G(\omega)kT_0 \tag{4-3}$$

where

$F(\omega)$ = the noise factor of the amplifier

$G(\omega)$ = the gain response of the amplifier

Knowing the transfer function $H(\omega)$ of the amplifier from the diode terminals to the output port, then the power spectral density of the current noise source is given by

$$S_y(\omega) = |H(\omega)|^2 S_i(\omega) \tag{4-4}$$

The mean square value of the generated noise current is

$$\langle I^2 \rangle = \frac{1}{2\pi} \int_{-\infty}^{\infty} S_i(\omega) d\omega \tag{4-5}$$

or

$$\langle I^2 \rangle = f(V) = \frac{1}{2\pi} \int_{-\infty}^{\infty} [F(\omega) - 1] \frac{G(\omega,V)}{|H(\omega)|^2} d\omega \tag{4-6}$$

where the gain is expressed as a function of frequency and voltage.

The noise figure of the Gunn Effect amplifier studied here was measured using the setup shown in Figure 32. The measurement analysis is performed by considering the block diagram of Figure 33. The losses from the output of the noise source to the amplifier input are idealized into a lossy network of net loss L_1 and noise factor F_A. The amplifier has a noise factor F_A and gain G_A. The losses from the output of the amplifier to the terminals of the mixer IF system are represented by a loss L_2 and noise factor F_2. When the amplifier is out of the measurement system, the measured overall noise factor is:

$$F_{ml} = F_1 + L_1(F_2 - 1) + L_1L_2(F_{mix} - 1) \qquad (4\text{-}7)$$

where F_{mix} is the noise factor of the mixer IF system. Assuming that the lossy networks are at the standard temperature of 290°K, then

$$F_1 = L_1$$
$$F_2 = L_2 \qquad (4\text{-}8)$$

So:

$$F_{ml} = L_1L_2F_{mix} \qquad (4\text{-}9)$$

When the amplifier is included, the measured overall noise factor is:

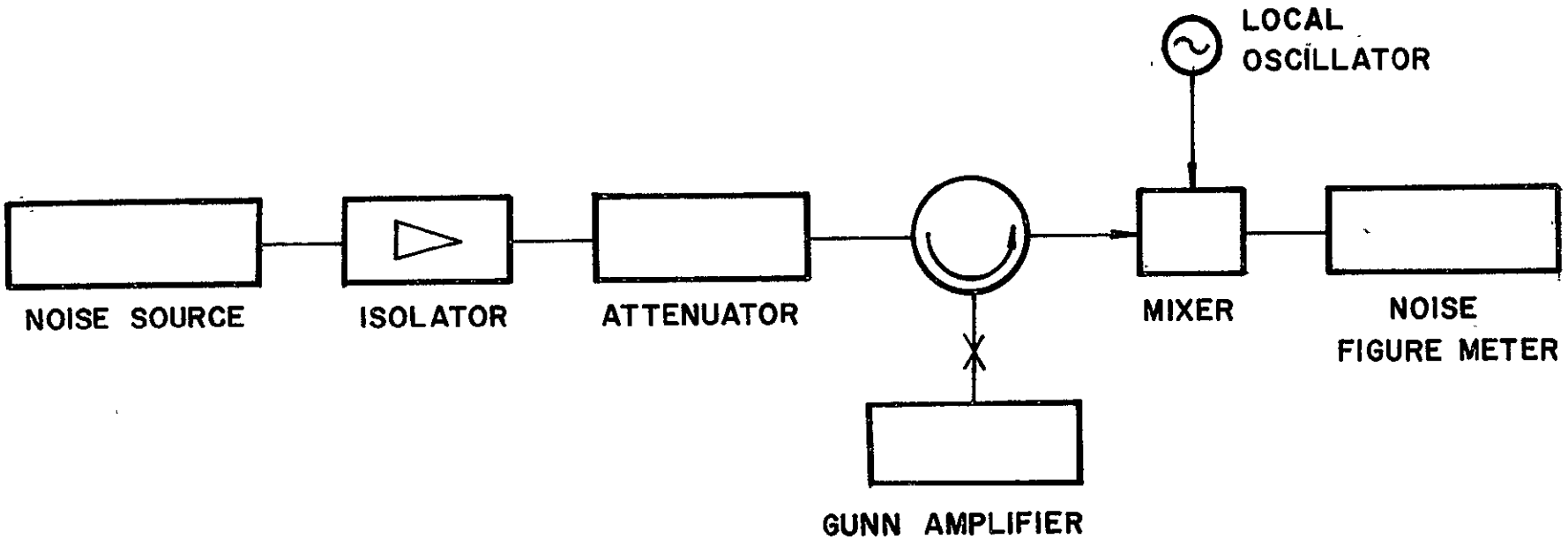

Figure 32. Noise Figure Setup

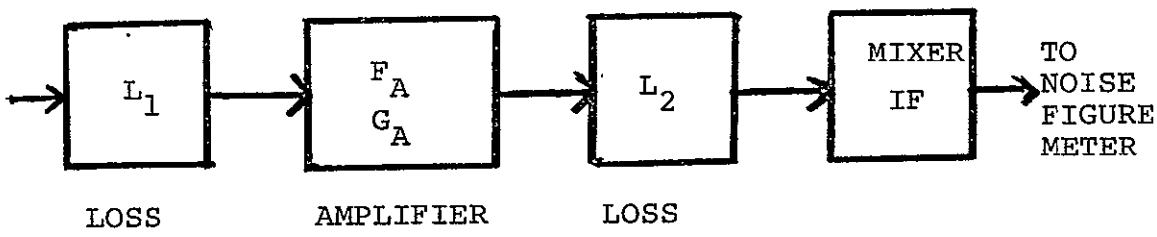

Figure 33. Noise Figure Calculation

$$F_{m2} = L_1 + L_1(F_A - 1) + \frac{L_1(L_2 - 1)}{G_A} + L_1L_2\,\frac{(F_{mix} - 1)}{G_A}$$

$$= L_1F_A + \frac{L_1L_2F_{mix}}{G_A} - \frac{L_1}{G_A} \qquad (4\text{-}10)$$

Substituting equation (4-9) into (4-10), we get

$$F_{m2} = L_1F_A + \frac{F_{m1}}{G_A} - \frac{L_1}{G_A} \qquad (4\text{-}11)$$

Thus the noise factor of the amplifier is

$$F_A = \frac{1}{L_1}\left(F_{m2} + \frac{L_1}{G_A} - \frac{F_{m1}}{G_A}\right) \qquad (4\text{-}12)$$

Expressing this result in decibels:

$$F_A = 10\,\log_{10}\left(F_{m2} + \frac{L_1}{G_A} - \frac{F_{m1}}{G_A}\right) - 10\,\log L_1 \qquad (4\text{-}13)$$

In our experiment, the loss, L_1, from the output flange of the noise source to the input plane of the amplifier was measured to be 2dB. With a short in front of the amplifier the system noise figure, F_{m1}, was 18.5dB. With the amplifier in the circuit, the measured noise figure was 27dB. The gain of the amplifier, biased at 5.85 volts, was found to be 10dB at a frequency of 8.74GHz. Using the above results in equation (4-13), the amplifier noise figure is then 24.98dB.

When the diode was stabilized and biased for broadband gain response, it was found that it generated 3μW of noise power. No coherent oscillations were detected on the spectrum analyzer. This broadband noise is likely due to the formation of space charge in the active layer of the Gunn

diode. Assuming that the noise generated by the diode is white, its power spectral density is 3.2×10^{-16} W/Hz over the waveguide bandwidth. In order to make the noise figure measurement, the operating point of the diode had to be optimized by varying the bias voltage and the tuning short circuit position until a power meter indicated 0μW on its 3μW scale. This resulted in a narrowband gain response centered at 8.74GHz. The high noise figure of the amplifier is due to the quality of diode used. With a good quality diode a noise figure ranging from 15 to 20dB can be realized (32).

5. CONCLUSIONS

5.1 PRINCIPAL RESULTS

It has been shown that Gunn Effect devices can be used as negative resistance amplifiers in three modes:

a. The subcritical and stable amplifier predicted by McCumber and Chynoweth and realized by Thim.

b. The traveling domain amplifier.

c. The supercritical amplifier first realized by Perlman.

In this work, supercritical amplifiers were built using waveguide circuitry. To stabilize the diode one needs to vary the bias voltage and the load on the diode. In this way broadband gains exceeding 10dB over a 1GHz band have been realized. Peak gains of 28dB have been demonstrated. In order to gain an insight into the operation of the waveguide amplifier, the equivalent circuit approach has been used. An equivalent circuit consisting of sections of waveguides and lumped elements was derived. The calculated VSWR response of the model of the transformer did not agree with the measurements. The discrepancy may be due to the step discontinuity reactances which have been neglected.

Using measurements of the gain and phase response, the dependence of the diode equivalent circuit parameters on voltage, temperature and input signal power has been found. The calculations show that the diode can be modeled as a negative resistance in series with a capacitive reactance.

The behavior of the gain response with bias voltage, temperature or input power can be explained by the dependence of the diode impedance on these parameters. In the stable region, the magnitude of the shunt negative resistance decreases with increasing voltage or temperature over a certain band of frequencies. This corresponds to an increase in gain, which continues until oscillations start. When biased at 6.5 volts, the calculated series negative resistance of the diode used is constant at -30Ω from 9.0 to 10.8GHz, at 7.0 volts it is flat at -45Ω from 9.2 to 10.2GHz. The reactance of the diode varies greatly with voltage, temperature and input power. However, no significant change of the negative resistance with input power has been detected over the range of input powers examined.

Using these results, a theoretical gain response has been calculated using both a constant negative resistance of -30Ω and a capacitance of 0.5pF. The calculations were shown to be in remarkable agreement with the experimental data at 6.5 volts. The phase response of the simulation had the same trends as the experimental one. Both were nonlinear at high frequencies and they tracked closely at midband. These results give greater confidence in the equivalent model used for the amplifier.

The Gunn diodes used in this work had a low power output. They begin to saturate at about -8dBm, but they have an extremely wide linear rnage. Amplification at 28dB

over a 94dB linear range has been measured. The phase linearity is good but exhibits nonlinearities at the upper end of the X-band. The noise figure of the amplifier was found to be 24dB at 10dB gain. With better constructed diodes, the performance of these amplifiers can be improved to the point where system applications are feasible. A noise figure of 15dB would be excellent given the inherent noisiness of the Gunn diode due to the formation of space charge.

5.2 FUTURE WORK

The work which has been presented herein can be extended in several ways:

a. With suitable diodes, reflection-type amplifiers can be built at millimeter wave frequencies.

b. The equivalent circuit used can be improved by taking into account the step discontinuity reactances of the transformer, the loading effect of the feedthrough circuit and the transformation of the electromagnetic field from a radial TEM mode around the diode to a TE_{10} mode at great distances away from it.

c. Because of the wideband nature of the amplifier studied, a circulator may not be the best way of coupling the amplifier to its load. Work should be done on the design of a transmission-type amplifier.

The Gunn diode costs very little to operate as compared to low power TWT's; this feature, plus improved performance, will enhance its use in systems applications.

6. ACKNOWLEDGEMENT

The author wishes to thank the African-American Institute for its support and the International Technology Development Center which sponsored this work through NASA Grant No. Y/NGL-26-008-054. He is grateful to the former Monsanto Microwave Group for generously providing the Gunn diodes.

7. APPENDICES

APPENDIX 7.1

Measurement of Gain-Phase Response

The gain of a reflection-type amplifier is given by the magnitude of the reflection coefficient, $|\Gamma|$. The phase of the reflection coefficient at a suitable reference plane gives the phase response of the amplifier. The setup of Figure 7-1 was used to measure $|\Gamma|$ and arg (Γ). The output of a square wave modulated microwave source is split up by a 10dB coupler. One part is attenuated by a factor of X, thus setting the input power to the amplifier. The other part of the source output, after additional attenuation by Y, is phase shifted and applied to one input of a magic Tee. The amplified signal is sampled by a 10dB coupler and also applied to the magic Tee. Then one looks for a null at the output of the E or H arm of the Tee. If the output is taken from the E arm, a null will be observed when the two inputs to the Tee are of equal magnitude and in phase. To get a reference phase, a short circuit is placed at the input of the amplifier and a broadband null is established by setting the attenuators and the phase shifter. If P_0 is the power output of the source, then from Figure 7-1-b the magnitude condition for a null gives:

$$\frac{P_0}{10Y} = \frac{9P_0G}{100X} \qquad (7\text{-}1\text{-}1)$$

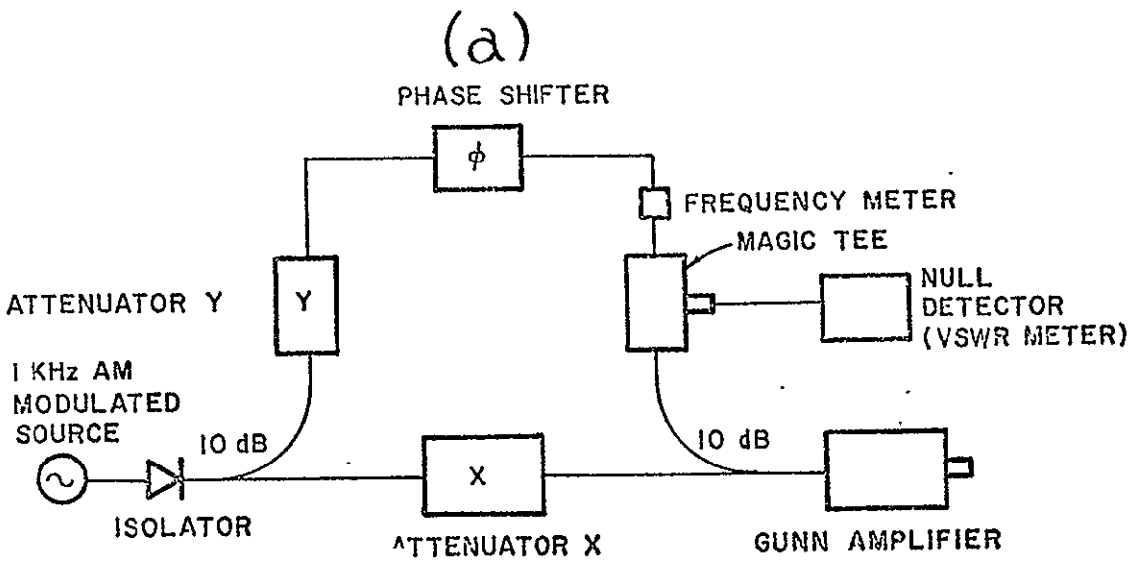

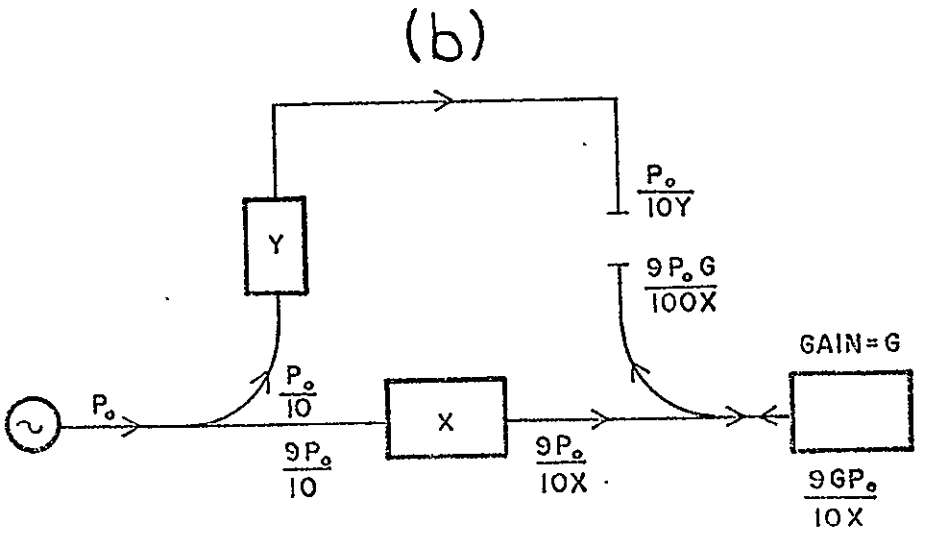

Figure 7.1.1. (a) Gain Phase Measurement Setup
(b) Gain Calculation

where G is the gain of the amplifier. Thus the power gain is:

$$G = \frac{10X}{9Y} \tag{7-1-2}$$

or in dB:

$$\begin{aligned} G_{dB} &= 10 \log\left(\frac{10}{9}\right) + X_{dB} - Y_{dB} \\ &= 0.47 + X_{dB} - Y_{dB} \end{aligned} \tag{7-1-3}$$

With a short circuit at the input of the amplifier, G = 0dB so the attenuators are set such that:

$$Y_{dB} = X_{dB} + 0.47 \tag{7-1-4}$$

The reference phase is calculated as follows by referring to Figure 7-1-2:

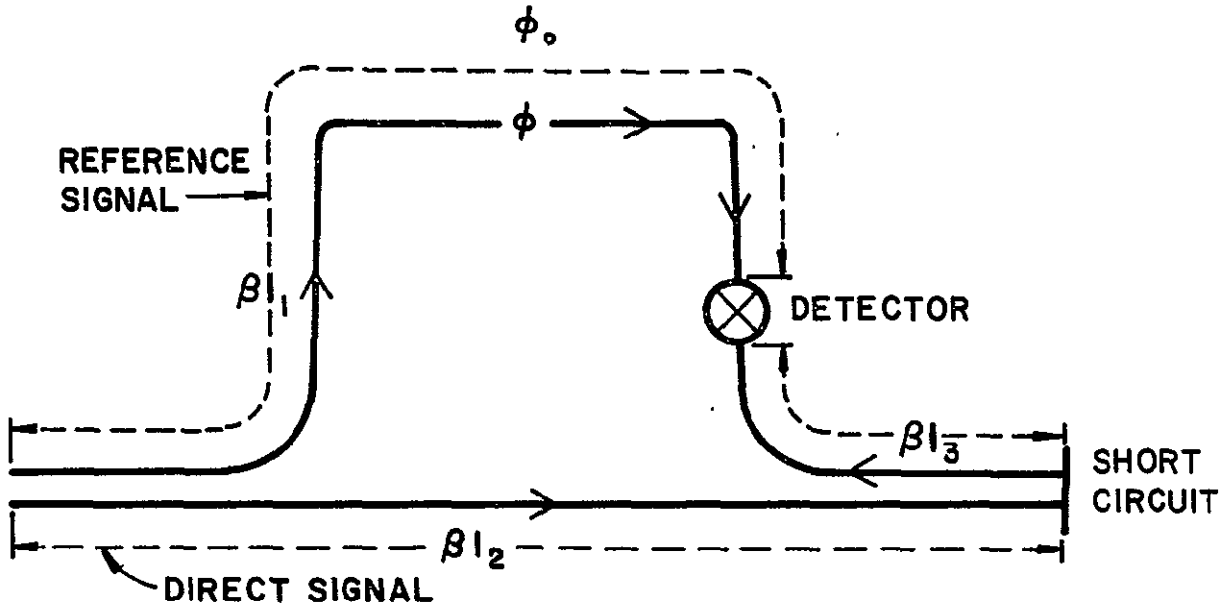

Figure 7-1-2. Reference Phase

Let ℓ_1 be the length of the waveguide circuitry from the isolator through the reference arm to the detector in the magic Tee. Then if ϕ_0 is the setting of the phase shifter which gives a broadband null, the phase shift of the reference signal at the detector will be

$$\beta\ell_1 + \phi_0 \tag{7-1-5}$$

Let ℓ_2 be the distance from the isolator to the short circuit, and ℓ_3 the distance from the short circuit to the detector, then the phase shift of the reflected signal at the detector is:

$$\beta\ell_2 + \beta\ell_3 \tag{7-1-6}$$

For a null, the phase condition is:

$$\beta\ell_1 + \phi_0 = \beta(\ell_2 + \ell_3) \tag{7-1-7}$$

or

$$\phi_0 = \beta(\ell_2 + \ell_3 - \ell_1) \tag{7-1-8}$$

With the amplifier in the circuit, the phase balance is changed by an amount ϕ_G, due to the amplifier. Then the phase shift of the reflected signal at the detector is:

$$\beta\ell_2 + \beta\ell_3 + \phi_G \tag{7-1-9}$$

For a null, the phase shifter has to be set at a new value ϕ_R, such that:

$$\beta\ell_2 + \beta\ell_3 + \phi_G = \beta\ell_1 + \phi_R \qquad (7\text{-}1\text{-}10)$$

Then the phase of the reflection coefficient at the input of the amplifier is:

$$\phi_G = \phi_R + \beta(\ell_1 - \ell_2 - \ell_3) \qquad (7\text{-}1\text{-}11)$$

From (7-1-8) we get:

$$\phi_G = \phi_R - \phi_0 \qquad (7\text{-}1\text{-}12)$$

Thus, using equations (7-1-3) and (7-1-12), one can get the gain and phase response of the amplifier.

APPENDIX 7.2

Input Impedance of Amplifier

Let Z be the input impedance of the amplifier, Z_c the characteristic impedance of the output waveguide. Then the reflection coefficient at the terminals of the amplifier is

$$\Gamma = \frac{Z - Z_c}{Z + Z_c} \tag{7-2-1}$$

Solving for Z, we get

$$Z = Z_c \frac{1 + \Gamma}{1 - \Gamma} \tag{7-2-2}$$

From the gain-phase measurement procedure of Appendix 7.1, we can write

$$\Gamma = |\Gamma| e^{i\psi} \tag{7-2-3}$$

where $|\Gamma|$ is related to the gain, ψ is the phase. Substitute (7-2-3) into (7-2-2):

$$\begin{aligned} Z &= Z_c \frac{1 + |\Gamma| e^{i\psi}}{1 - |\Gamma| e^{i\psi}} \\ &= Z_c \frac{1 + |\Gamma|\cos\psi + i|\Gamma|\sin\psi}{1 - |\Gamma|\cos\psi - i|\Gamma|\sin\psi} \end{aligned} \tag{7-2-4}$$

Rationalizing equation (7-2-4), we get

$$\begin{aligned} Z = {} & Z_c \frac{1 - |\Gamma|^2}{1 + |\Gamma|^2 - 2|\Gamma|\cos\psi} \\ & + iZ_c \frac{2|\Gamma|\sin\psi}{1 + |\Gamma|^2 - 2|\Gamma|\cos\psi} \end{aligned} \tag{7-2-5}$$

Then if $Z = R + jX$, we get

$$R = Z_c \frac{1 - |\Gamma|^2}{1 + |\Gamma|^2 - 2|\Gamma|\cos\psi} \tag{7-2-6}$$

$$X = \frac{2Z_c|\Gamma|\sin\psi}{1 + |\Gamma|^2 - 2|\Gamma|\cos\psi} \tag{7-2-7}$$

APPENDIX 7.3

Diode Equivalent Circuit

Consider the general network in Figure 7-1-b, terminated with a load impedance Z_L:

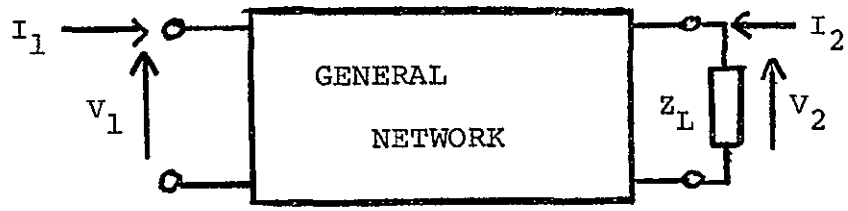

Figure 7.3.1. General Network

A set of voltage and current coordinates can be defined in terms of the A-matrix of the network:

$$\begin{bmatrix} V_1 \\ I_1 \end{bmatrix} = \begin{bmatrix} a_{11} & a_{12} \\ a_{21} & a_{22} \end{bmatrix} \begin{bmatrix} V_2 \\ -I_2 \end{bmatrix} \qquad (7\text{-}3\text{-}1)$$

The input impedance of the network is given by

$$Z_{in} = \frac{V_1}{I_1} = \frac{a_{11}V_2 - a_{12}I_2}{a_{21}V_2 - a_{22}I_2} \qquad (7\text{-}3\text{-}2)$$

But the load impedance is given by

$$Z_L = -\frac{V_2}{I_2} \qquad (7\text{-}3\text{-}3)$$

So:

$$Z_{in} = \frac{a_{11}Z_L + a_{12}}{a_{21}Z_L + a_{22}} \qquad (7\text{-}3\text{-}4)$$

Solving Z_L in terms of Z_{in}, we get

$$Z_L = \frac{a_{12} - a_{22}Z_{in}}{a_{21}Z_{in} - a_{11}} \qquad (7\text{-}3\text{-}5)$$

The load admittance is then:

$$Y_L = \frac{1}{Z_L} = \frac{a_{21}Z_{in} - a_{11}}{a_{12} - a_{22}Z_{in}} \qquad (7\text{-}3\text{-}6)$$

Thus, if one knows Z_{in} and the terms of the A-matrix of the network, one can calculate the output admittance. In general we have

$$\begin{aligned} Z_{in} &= R + jX \\ a_{11} &= h_1 + jh_2 \\ a_{12} &= k_1 + jk_2 \\ a_{21} &= \ell_1 + k\ell_2 \\ a_{22} &= m_1 + jm_2 \end{aligned} \qquad (7\text{-}3\text{-}7)$$

Substitute equation (7-3-7) into equation (7-3-6):

$$Y_L = \frac{(\ell_1 + j\ell_2)(R + jX) - h_1 - jh_2}{k_1 + jk_2 - (m_1 + jm_2)(R + jX)} \qquad (7\text{-}3\text{-}8)$$

$$Y_L = \frac{R\ell_1 - X\ell_2 - h_1 + j(R\ell_2 + X\ell_1 - h_2)}{k_1 - m_1R + m_2X + j(k_2 - m_2R - m_1X)}$$

Let,

$$\begin{aligned} A &= R\ell_1 - X\ell_2 - h_1 \\ B &= R\ell_2 + X\ell_1 - h_2 \\ C &= k_1 - m_1R + m_2X \\ D &= k_2 - m_2R - m_1X \end{aligned}$$

Then

$$Y_L = \frac{(A + jD)(C - jE)}{C^2 + E^2} = \frac{AC + DE + j(DC - AE)}{C^2 + E^2} \quad (7\text{-}3\text{-}10)$$

but

$$Y_L = G + jB$$

Then

$$G = \frac{AC + DE}{C^2 + E^2}$$

$$B = \frac{DC - AE}{C^2 + E^2} \quad (7\text{-}3\text{-}11)$$

Thus, using the results of Appendix 7.1, one can calculate the equivalent circuit of the diode from gain and phase data.

APPENDIX 7.4

Calculation of the A-Matrix of the Microwave Circuit

The lumped element equivalent network of the diode mount is shown below:

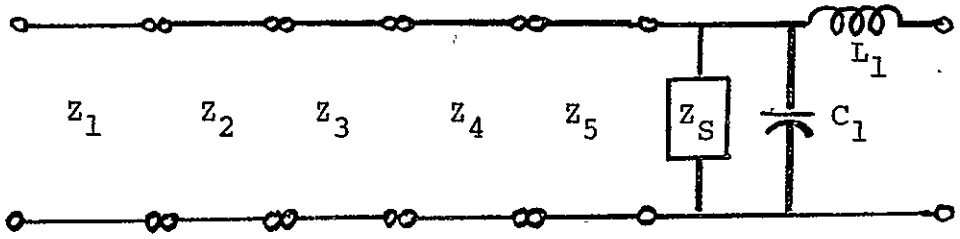

The stepped impedance transformer is modeled as a cascade of transmission lines. L_1, C_1 represent the inductance and capacitance associated with the package of the diode. It is well known from circuit theory that the overall A-matrix of a cascade of network elements is the products of their individual A-matrices in the order of their physical position in the network.

The A-matrix representation of a lossless transmission line of length $\ell = d$ and whose characteristic impedance Z_0 is:

$$[A] = \begin{bmatrix} \cos(\beta d) & jZ_0 \sin\beta d \\ \frac{j\sin\beta d}{Z_0} & \cos\beta d \end{bmatrix}$$

So the overall A-matrix is:

$$\begin{bmatrix} \cos\beta\ell_5 & jZ_{0_5}\sin\beta\ell_5 \\ \frac{j\sin\beta\ell_5}{Z_{0_5}} & \cos\beta\ell_5 \end{bmatrix} \begin{bmatrix} \cos\beta\ell_4 & jZ_{0_4}\sin\beta\ell_4 \\ \frac{j\sin\beta\ell_4}{Z_{0_4}} & \cos\beta\ell_4 \end{bmatrix}$$

times

$$\begin{bmatrix} \cos\beta\ell_3 & jZ_{0_3}\sin\beta\ell_3 \\ \frac{j\sin\beta\ell_3}{Z_{0_3}} & \cos\beta\ell_3 \end{bmatrix} \begin{bmatrix} \cos\beta\ell_2 & jZ_{0_2}\sin\beta\ell_2 \\ \frac{j\sin\beta\ell_2}{Z_{0_2}} & \cos\beta\ell_2 \end{bmatrix}$$

times

$$\begin{bmatrix} \cos\beta\ell_1 & jZ_{0_1}\sin\beta\ell_1 \\ \frac{j\sin\beta\ell_1}{Z_{0_1}} & \cos\beta\ell_1 \end{bmatrix} \begin{bmatrix} 1 & 0 \\ \frac{1}{jZ_{0_1}\tan\beta d} & 1 \end{bmatrix} \begin{bmatrix} 1 & 0 \\ j\omega C_1 & 1 \end{bmatrix} \begin{bmatrix} 1 & j\omega L_1 \\ 0 & 1 \end{bmatrix}$$

8. BIBLIOGRAPHY

1. Kroemer, H., "Proposed Negative Mass Microwave Amplifier", Physical Review 109, p. 1856, March 1958.

2. Kroemer, H., "The Physical Principles of a Negative-Mass Amplifier", Proceedings of the IEEE 47, pp. 397-406, March 1959.

3. Ridley, B. K., and T. B. Watkins, "The Possibility of Negative Resistance Effects in Semiconductors", Proceedings of the Physical Society (London) 78, pp. 293-304, August 1961.

4. Hilsum, C., "Transferred Electron Amplifiers and Oscillators", Proceedings of the IRE 50, pp. 185-189, February 1962.

5. Gunn, J. B., "Microwave Oscillations of Current in III-V Semiconductors", Solid State Communications 1, pp. 88-91, September 1963.

6. Gunn, J. B., "Instabilities of Current and of Potential Distribution in GaAs and InP", Plasma Effects in Solids (Paris, 1964), p. 199, Paris: Dunod, 1965.

7. Kroemer, H., "Theory of the Gunn Effect", Proceedings of the IEEE (Correspondence) 52, p. 1736, December 1964.

8. Hutson, A. R., A. Jayaraman, A. G. Chynoweth, A. S. Coriell, and W. L. Feldman, "Mechanism of the Gunn Effect from a Pressure Experiment", Physical Review Letters 14, pp. 639-641, April 19, 1965.

9. Allen, J. W., Shyam, M., Chen, Y. S., and Pearson, G. L., "Microwave Oscillations in $GaAs_xP_{1-x}$ Alloys", Applied Physics Letters 7, pp. 78-80, August 1965.

10. Tsai, Wei-Ching, "The Characteristics and Applications of Gunn Effect Devices", Ph. D. dissertation, Department of Electrical Engineering, Washington University, July 1969.

11. McCumber, D. E., and A. G. Chynoweth, "Theory of Negative Conductance Amplification and of Gunn Instabilities in 'Two-Valley' Semiconductors", IEEE Transactions on Electron Devices ED-13, pp. 4-21, January 1966.

12. Morse and Feshbach, Methods of Theoretical Physics, Part I, p. 372.

13. Kroemer, H., "Negative Conductance in Semiconductors", IEEE Spectrum 5, pp. 47-56, January 1968.

14. Narayan, S. V., and F. Sterzer, "Transferred Electron Amplifiers and Oscillators", IEEE Transactions on Microwave Theory and Techniques MTT-18, No. 11, pp. 773-783, November 1970.

15. Tsai, W. C., and F. J. Rosenbaum, "Bias Circuit Oscillations in Gunn Devices", IEEE Transactions on Electronic Devices ED-16, No. 2, pp. 196-202, February 1969.

16. Uenohara, M., "Microwave Amplification in a Bulk Semiconductor", Applied Physics Letters 7, p. 117, September 1965.

17. Thim, H. W., and M. R. Barber, "Microwave Amplification in a GaAs Bulk Semiconductor", IEEE Transactions on Electron Devices ED-13, No. 1, pp. 110-114, January 1966.

18. Foyt, A. G., and T. M. Quist, "Bulk GaAs Microwave Amplifiers", IEEE Transactions on Electron Devices ED-13, No. 1, p. 199 (correspondence), January 1966.

19. Hakki, B. W., and S. Knight, "Microwave Phenomena in Bulk GaAs", IEEE Transactions on Electron Devices, ED-13, No. 1., pp. 94-105, January 1966.

20. McWhorter, A. L., and A. G. Foyt, "Bulk GaAs Negative Conductance Amplifiers", Applied Physics Letters 9, No. 8, pp. 300-302, October 15, 1966.

21. Thim, H. W., "Temperature Effects in Bulk GaAs Amplifiers", IEEE Transactions on Electron Devices ED-14, No. 2, pp. 59-62, February 1967.

22. Hakki, B. W., and J. P. Beccone, "Microwave Negative Conductance of Bulk GaAs", IEEE Proceedings 54, No. 6, pp. 916-917, June 1966.

23. Hobson, G. S., Electronics Letters 2, p. 207, 1966.

24. Heinle, W., "On the Equivalent Circuit of a Gunn Diode", International Journal of Electronics 23, No. 6, pp. 541-546, 1967.

25. Thim, H. W., "Linear Negative Conductance Amplification with Gunn Oscillators", Proceedings of the IEEE 55, No. 3, pp. 446-447, March 1967.

26. Thim, H. W., "Linear Microwave Amplification with Gunn Oscillators", IEEE Transactions on Electron Devices ED-14, pp. 517-522, September 1967.

27. Carroll, J. E., Electronics Letters 2, p. 215, 1966.

28. Narayan, S. V., and F. Sterzer, "Stabilization of Transferred Electron Amplifiers with Large n_0L Products", Electronics Letters 5/2, p. 30, January 1969.

29. Perlman, B. S., T. E. Walsh, and R. E. Enstrom, "Stabilized Supercritical Transferred Electron Amplifiers", IEEE Journal of Solid State Circuits SC-4, No. 6, pp. 374-376, December 1969.

30. Magarshack, J., and A. Mircea, "Wideband CW Amplification in X-Band with Gunn Diodes", IEEE International Solid State Circuits Conference, Philadelphia, February 1970.

31. Ibid.

32. Perlman, B. S., "CW Microwave Amplification from Circuit Stabilized Epitaxial GaAs Transferred Electron Devices", ISSCC, Philadelphia, February 1970.

33. Young, L., "Tables for Cascaded Homogeneous Quarter-Wave Transformers", IRE Transactions on Microwave Theory and Techniques MTT-7, pp. 233-237, April 1959.

34. Roe, J. M., and F. J. Rosenbaum, "Characterization of Packaged Microwave Diodes in Reduced Height Waveguide", IEEE Transactions on Microwave Theory and Techniques MTT-18, pp. 638-642, September 1970.

35. Roe, J. M., "The Packaged and Mounted Microwave Diode in Reduced Height Waveguide", Master's Thesis, Washington University, June 1969.

36. Fano, R. M., "Theoretical Limitations on the Broadband Matching of Arbitrary Impedances", Journal of the Franklin Institute 249, pp. 57-84, 139-54, January-February 1950.

37. Bode, H. W., Network Analysis and Feedback Amplifier Design, pp. 360-371, D. Van Nostrand Co., New York 1945.

38. Youla, D. C., and L. I. Smilen, "Optimum Negative-Resistance Amplifiers", Proceedings of the Symposium on Active Networks and Feedback Systems, Polytechnic Institute of Brooklyn, 1960.

39. Paley, R. E. A. C., and N. Wiener, "Fourier Transforms in the Complex Domain", American Mathematics Society Colloquium Publications 19, pp. 16-17, 1934.

40. Matthei, G. L., L. Young and E. M. T. Jones, Microwave Filters, Impedance-Matching Networks, and Coupling Structures, McGraw-Hill, New York, 1964.

41. Gledhill, C. S., and A. M. H. Issa, "Exact Solutions of Stepped Impedance Transformers having Maximally Flat and Chebychev Characteristics", IEEE Transactions on Microwave Theory and Techniques MTT-17, No. 7, pp. 379-386, July 1969.

42. Garbrecht, K., and W. Heinlein, "A Simple Broad-Banding Technique for Microwave Reflection-Type Amplifiers", Microwave Journal, pp. 77-84, February 1970.